Official Journal of CIOMP
elight.springeropen.com

REVIEW

Open Access

Interdisciplinary advances in microcombs: bridging physics and information technology

Bai-Cheng Yao[1*†], Wen-Ting Wang[2†], Zhen-Da Xie[3], Qiang Zhou[4], Teng Tan[1], Heng Zhou[1], Guang-Can Guo[4,5], Shi-Ning Zhu[3], Ning-Hua Zhu[2] and Chee Wei Wong[6*]

Abstract

The advancement of microcomb sources, which serve as a versatile and powerful platform for various time–frequency measurements, have spurred widespread interest across disciplines. Their uses span coherent optical and microwave communications, atomic clocks, high-precision LiDARs, spectrometers, and frequency synthesizers. Recent breakthroughs in fabricating optical micro-cavities, along with the excitation and control of microcombs, have broadened their applications, bridging the gap between physical exploration and practical engineering systems. These developments pave the way for pioneering approaches in both classical and quantum information sciences. In this review article, we conduct a thorough examination of the latest strategies related to microcombs, their enhancement and functionalization schemes, and cutting-edge applications that cover signal generation, data transmission, quantum analysis, and information gathering, processing and computation. Additionally, we provide in-depth evaluations of microcomb-based methodologies tailored for a variety of applications. To conclude, we consider the current state of research and suggest a prospective roadmap that could transition microcomb technology from laboratory settings to broader real-world applications.

1 Introduction

Generally, a frequency comb is comprised of a series of spectral lines that are spaced across the spectrum after phase-locking between each other [1, 2]. These spectral lines are typically produced by a laser after modulation, and they represent a multitude of discrete frequencies that are evenly distributed and maintain a precise interrelationship, often characterized by a consistent interval between frequencies. The generation of a stable frequency comb (e.g. soliton) is achieved via mode-locking, a technique that aligns the various modes of a laser to produce a sequence of coherent, ultra-short pulses [3]. The exactitude and steadiness of the frequency comb's spectral lines render it an invaluable instrument for numerous scientific and technological endeavors [4]. Over the past decades, frequency combs have been instrumental in transforming areas like precision spectroscopy, metrology, and optical frequency synthesis [5]. Their capacity for ultra-precise time and frequency measurements has beneficial implications for atomic

†Bai-Cheng Yao and Wen-Ting Wang have contribute equally to this work.

*Correspondence:
Bai-Cheng Yao
yaobaicheng@uestc.edu.cn
Chee Wei Wong
cheewei.wong@ucla.edu
[1] Key Laboratory of Optical Fibre Sensing and Communications (Education Ministry of China), University of Electronic Science and Technology of China, Chengdu 611731, China
[2] Communication and Integrated Photonics Laboratory, Xiong'an Institute of Innovation, Chinese Academy of Sciences, Xiong'an 071700, China
[3] National Laboratory of Solid State Microstructures and, School of Electronic Science and Engineering, School of Physics and College of Engineering and Applied Sciences, Nanjing University, Nanjing 210008, China
[4] Institute of Fundamental and Frontier Sciences, University of Electronic Science and Technology of China, Chengdu 610054, China
[5] CAS Key Laboratory of Quantum Information, University of Science and Technology of China, Hefei 230026, China
[6] Fang Lu Mesoscopic Optics and Quantum Electronics Laboratory, University of California, Los Angeles, CA 90095, USA

clocks, telecommunications, and research in fundamental physics.

Since the 1990s, the push for compact and portable frequency comb devices has been a significant driver in their evolution [6]. The trend has progressed from large, room-scale apparatuses to more manageable table-top versions, with the ultimate goal of developing chip-scale iterations [7]. Besides external cavity modulation [8], a prominent innovation in this journey is the Kerr frequency comb, produced within optical micro-cavities—also known as microcombs [9]. Kerr frequency combs derive their name from the Kerr effect, a third-order nonlinear optical phenomenon occurring in optical microresonators [10]. This effect describes how the refractive index of a material varies in response to the intensity of incoming light. As the light's intensity alters, it leads to self-interaction within the light waves, which can generate a broad spectrum of new optical frequencies. Since 2014, the realization of dissipative soliton Kerr combs enable low noise state with evenly spaced optical lines [11]. Besides, mode-locked dark pulse Kerr combs in normal-dispersion microresonators also demonstrate high coherence [12]. Furthermore, octave-spanning of a microcomb [13] offers a way to lock not only the repetition, but also the carrier-envelope offset, providing the elements to precisely determine all frequency comb lines [14]. Up to now, versatile frequency combs play an instrumental role in a multitude of domains, including precision metrology for highly accurate measurements, telecommunications for improved data transmission, and spectroscopy for detailed chemical analysis.

Microcomb technology, thanks to its expanding capabilities in spectral bandwidth, energy efficiency, phase coherence, and stability, is driving a multitude of new mechanisms, innovative platforms, and groundbreaking applications [15]. Figure 1 demonstrates its platforms and applications in schematics. It also inspires interdisciplinary progress such as active–passive heterogeneous integration [16] and complex photonic system incorporation [17]. Moreover, in fields like microwave photonics, optical communications, precision measurements, neuromorphic computing, and quantum optics, the technology can also play a critical role. With its unique attributes, the microcomb has become an essential tool for frequency synthesis, spectrum filtering, signal processing, and improving the performances of optical communication and sensing systems.

Its versatility extends further, enabling precise timing, environmental detection, and the creation of highly efficient light sources, highlighting its potential to transform various scientific and industrial sectors. For instance, in spectroscopy, the optical frequency comb excels at precisely analyzing the structures of atoms and molecules [18]; in metrology, it delivers unparalleled accuracy in time and frequency measurements, which is vital for the development of next-generation atomic clocks and enhancing Global Positioning System (GPS) performance [19]; in telecommunications, microcombs are harnessed to boost the data transmission rate when combined with wavelength division multiplexing technology [20]; moreover, microcombs find applications in novel areas such as astronomical spectroscopy for exoplanet detection and

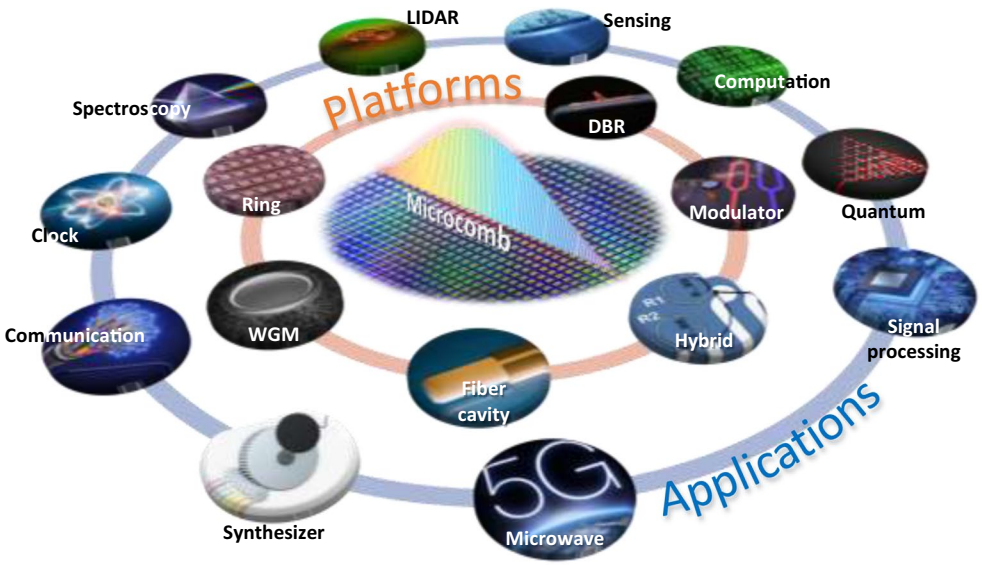

Fig. 1 Overview of microcombs. Microcombs can be formed in platforms ranging from on-chip microresonators, whispering gallery mode microcavities to modulators, and can be applied in versatile applications

in medical imaging, where they offer new prospects for non-invasive diagnostics [21]. The adaptability of microcombs across diverse disciplines underscores their potential as a transformative tool, promoting advancements in both scientific knowledge and technical advances.

In this review article, we provide a comprehensive introduction to the cross-disciplinary frontiers of microcombs, spanning from physical advances to technical applications. Specifically, our emphasis lies on the potential of microcombs in the field of information science. The article is structured as follows: Sect. 2 delves into the physical innovations encompassing microcavity materials and platforms, as well as the generation and functionalization schemes of microcombs. Section 3 to Sect. 5 explores advanced applications based on microcombs, with a primary focus on signal generation, information acquisition, data delivery, and signal processing. Section 6 presents a discussion on the distinctive characteristics of various microcombs, analyzing their advantages, limitations, and suitable application scenarios. This article concludes with an outlook on the technology of microcombs, highlighting its burgeoning development and potential to garner attention from a broad range of fields in and beyond photonics and optics.

2 Advances of generation and functionalization of microcombs

2.1 Emerging material platforms for microcomb generation

The development and enhancement of microcomb technology are fundamentally linked to the advancements in novel materials and structural platforms within the realm of microcavity photonics [13, 22]. The generation of frequency combs hinges on several key parameters, including the refractive index, *Q*-factor, nonlinear coefficient, chromatic dispersion, thermo-optic coefficient, and transparency spectrum [23]. These essential physical properties jointly influence the characteristics of microcombs, such as the frequency range, optical power, temporal behavior, and noise levels [24]. To date, numerous materials and cavity geometries have been investigated for their ability to form microcombs through nonlinear oscillations [25]. The array of materials used for crafting microresonators consists of silica (SiO_2), fluorides like magnesium fluoride (MgF_2), silicon nitride (Si_3N_4), aluminum nitride (AlN), lithium niobate ($LiNbO_3$), and highly-nonlinear III-V compounds (e.g. GaN, GaP and AlGaAs), to name a few. Correspondingly, various structural platforms including planar microrings, whispering gallery mode microresonators and fiber Fabry–Perot microcavities have been manufactured. These structures can generally be classified into three categories: on-chip rings, whispering gallery mode (WGM) cavities, and fiber resonators. As illustrated in Fig. 2a, researchers have developed unique strategies to merge these materials with geometric structures effectively. The extensive array of material-structure pairings has led to the creation of a multitude of versatile configurations that cater to diverse applications and performance requirements.

Silica (SiO_2), with a refractive index of approximately 1.44, is the most commonly used material for creating microresonators and has been widely applied in frequency comb generation (as shown in Fig. 2b) [9]. This material features an extensive transparency window that spans from the visible (VIS) to the mid-infrared (MIR) bands. While silica offers a relatively low third-order nonlinear coefficient ($n_2 \approx 2.6\times10^{-20}$ m^2W^{-1}), the formation of combs in passive SiO_2 cavities typically requires either a high input power or a microresonator with a high quality (*Q*) factor, which is defined as $Q=\omega/\Delta\omega$, wherein $\omega/2\pi$ and $\Delta\omega/2\pi$ are the central frequency and linewidth of the optical resonance. Usually, the total *Q* factor is related to the intrinsic and the coupling *Q* factors via the relation ${Q_{total}}^{-1}={Q_{intrisic}}^{-1}+{Q_{coupling}}^{-1}$. For instance, when the pump power introduced into the system is less than 100 mW, silica microcavities theoretically need *Q* factors on the order of 10^7 to generate microcombs [26]. However, reducing losses in silica microcavities is achievable. Recent reports indicate that silica microcavities can achieve Q factors as high as 4×10^9, which has enabled amplifier-free excitation [27]. In practice, silica-based microresonators are available in various configurations, with fiber microcavities and whispering gallery mode (WGM) microcavities being the most popular due to their adaptable design and ease of fabrication. To enhance nonlinearity in silica, high-index doped silica materials such as Hydex ($n=1.5$–1.9) have been developed [28]. These materials maintain low linear loss (typically < 5 dB/m) while offering significantly increased nonlinearity ($n_2=1.15\times10^{-19}$ m^2W^{-1}, approximately five times that of standard silica) without suffering from multiphoton absorption effects. Since 2010, high-performance microcombs have been successfully demonstrated in Hydex microrings [29], marking a critical advancement in integration. Another important group of materials for comb generation is fluorides, with magnesium fluoride (MgF_2, $n \approx 1.37$) being the first fluoride used for soliton microcomb production [30]. MgF_2 enables light transmission from the ultraviolet (~160 nm) to the MIR (~7 μm) band, yet its nonlinearity ($n_2 \approx 1\times10^{-20}$ m^2W^{-1}) is even lower than that of silica. Nonetheless, the impact of the low nonlinearity is mitigated by the material's extremely low optical loss, allowing ultra-high *Q* factors (ranging from 10^8 to 10^{10}) to be realized in fluoride-based microresonators [31], facilitating efficient comb formation (refer to Fig. 2c). Fluorides are typically shaped into mechanical polished WGM structures as they are challenging to fabricate using melt plasticity or photolithography techniques.

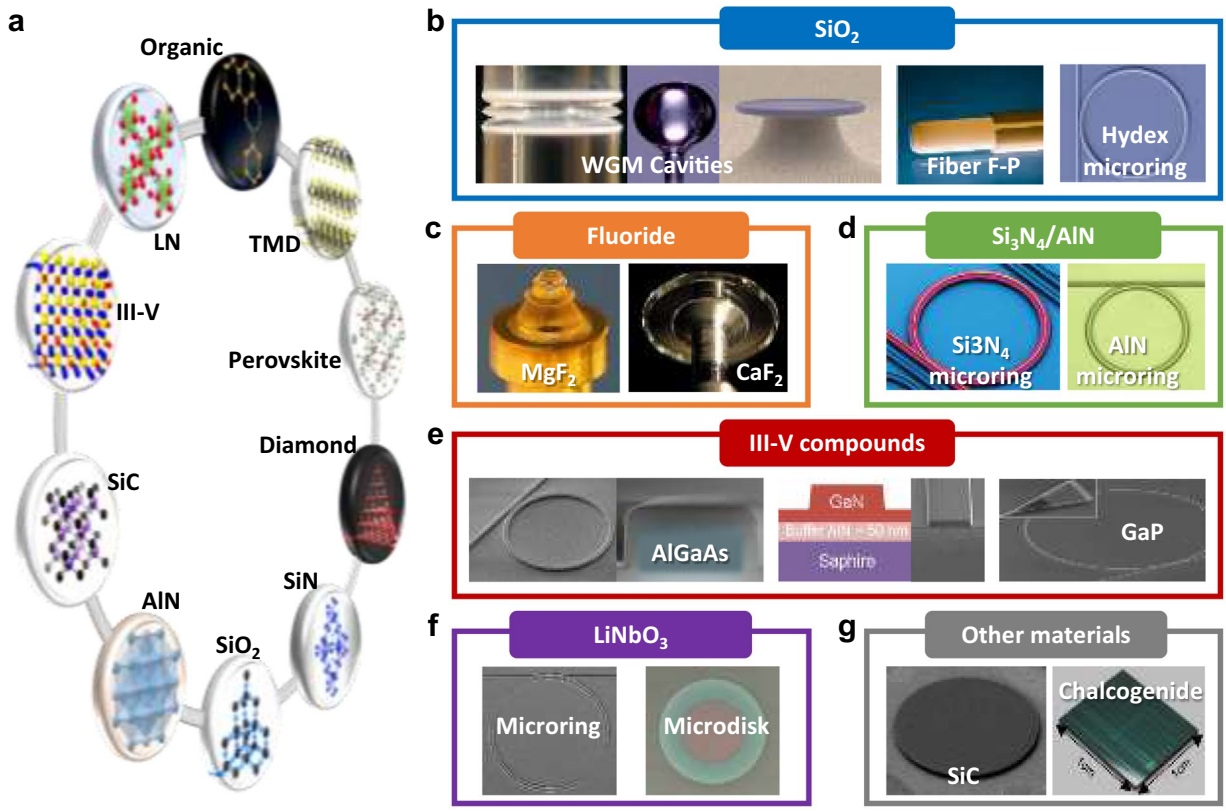

Fig. 2 Material and structural platforms for microcomb generation. **a**, Various materials for microcavity preparation. **b–f**, Pictures of microresonators based on diverse materials [9, 28, 30, 32, 35, 43, 50, 51, 55, 85, 98]. Specifically, microrod [32], microsphere [35], microtoroid [9], F-P [85] are fabricated using Hydex [28], MgF_2 [30], CaF_2, Si_3N_4 [98], AlN [43], $LiNbO_3$ [50, 51], III-V compounds [45–47] and Others [55]

In silica and fluoride-based WGM cavities, it is possible to adjust the mode numbers and mode volumes by fine-tuning the cavity size and geometry. Microtoroids and microrods, when crafted from the same substance, exhibit comparable Q factors, around 10^8. These are typically shaped using a thermal reflow process [32]. Microdisks, on the other hand, facilitate single-mode operation but are often produced through chemical etching techniques. Their free spectral range can cover from tens of GHz [33] to greater than 100 GHz [34], and they can reach high Q factors up to 10^9. One advantage of this design is the ability to control wedge angles, which permits versatile dispersion manipulation. Lastly, microspheres can be produced with a relatively straightforward approach, such as melting in a fiber splicer [35], and have demonstrated the highest Q factors to date, up to 10^{10} [36]. They support a wide variety of mode families and have a unique capability for inducing mode crossing and mode splitting [37], making the microsphere cavity an important platform for exploring physics that is independent of modes and for realizing intricate comb outputs.

Silicon nitride (Si_3N_4, with a refractive index $n \approx 1.98$) began capturing the interest of scientists for microcomb formation around 2010 [38], quickly establishing itself as a prime candidate due to its inherent physical properties such as a lack of Brillouin scattering [39] and compatibility with CMOS technology (refer to Fig. 2d). As of now, Si_3N_4 is the most commonly used material for fabricating on-chip microring resonators, boasting a strong third-order nonlinearity (with $n_2 \approx 2.5\times10^{-19}$ m^2W^{-1}). Typically, the Q factor of silicon nitride cavities highly depends on the device design, fabrication and optical band in measurement [40]. Recently, using a geometry enabling tightly confined mode, the Q factor of a Si_3N_4 microresonator exceeds 3×10^7 [17, 41]. While in cases where a low confined mode guided by nitride is present, the Q value can reach 10^8 or even higher [42]. On the other hand, since Si_3N_4 exhibits normal dispersion within the near-infrared (NIR) spectrum, it becomes essential to intricately design the microrings' structural dispersion to satisfy the phase-matching requirements necessary for soliton generation. Aluminum nitride (AlN) is a non-centrosymmetric material with a refractive index

of approximately 1.98, exhibiting both second and third order nonlinear optical properties characterized by $\chi^{(2)}$ and $\chi^{(3)}$ [43]. It stands as an ideal candidate for generating microcombs, primarily within the visible to near-infrared (NIR) spectrum, as illustrated in Fig. 2d. AlN's third order nonlinearity ($n_2 \approx 3\times10^{-19}$ m^2W^{-1}) is on par with that of Si_3N_4, while its thermal conductivity is remarkably high (around 285 W/m K), which greatly benefits heat management and fortifies the durability of optical microcombs under high optical powers. Additionally, AlN exhibits piezoelectric tunability, a key feature for providing dynamic feedback [44]. Besides AlN, there are more and more III–V compounds suitable for microcomb excitation due to their naturally high nonlinearity, as Fig. 2e shows. For instance, AlGaAs and its alloys boast substantial nonlinear effects that facilitate the formation of combs at ultra-low thresholds [45]. And, in a GaN microring, scientists obtained an intrinsic Q factor over 2.5 million, and extracted a nonlinear index $n_2 \approx 1.4\times10^{-18}$ m^2W^{-1} at telecom band [46]. Furthermore, the nonlinear index of a GaP microring at telecommunication wavelengths can reach 1.1×10^{-17} m^2W^{-1} [47]. Recently, AlGaAs microrings based soliton microcombs have been achieved successively in under cryogenic [48] and room temperature [49].

In pursuit of further enhancement of nonlinear coefficients within microcavities, while also ensuring on-chip integration compatibility, lithium niobate emerges as a suitable alternative [50, 51] (see Fig. 2f). This material boasts exceedingly high values for both $\chi^{(2)}$ and $\chi^{(3)}$ coefficients in broadband [52]. The first $LiNbO_3$ microring cavity was successfully fabricated in 2007 through benzocyclobutene bonding and photolithographic techniques [53]. Since then, $LiNbO_3$ microcavities have achieved Q factors of up to 10^7 [54], and the implementation of self-starting Kerr soliton microcombs in these structures has been accomplished [50].

Beyond the materials previously mentioned, a plethora of options have emerged for microcomb excitation as illustrated in Fig. 2g. Silicon carbide is notable for its ultra-wide transparency window ranging from 0.37 to 5.6 μm [55], while diamond membranes offer a substantial bandgap coupled with a minimal photonic absorption ratio [56]. In addition, chalcogenide glass (e.g. S, Se and Te compounds) is appropriate for mid-infrared and even longer wavelengths [57], and halide perovskites are also gaining attention for their compatibility with CMOS manufacturing processes [58], while two-dimensional materials are being explored for their potential to enhance photon-electron interactions [59–61]. In a groundbreaking study at 2020, Keskekler and colleagues proposed the generation of microcombs via induced symmetry breaking in graphene drums [62]. Complementing these material developments, innovative microresonator structures have been introduced: deformed microcavities for the generation of ultrawide microcombs [63], edgeless photonic crystal resonators for inducing spontaneous soliton formation [64], and microspheres with optical gain assistance to boost microcomb output. Specifically, in a microcavity, the resonant frequencies of a longitude mode μ (the relative mode number corresponding to the pumped mode ω_0) is written in:

$$\omega_\mu = \omega_0 + D_1\mu + \frac{1}{2}D_2\mu^2 + \frac{1}{6}D_3\mu^3 + \cdots \tag{1}$$

In this equation, $D_1/2\pi$ presents the free spectral range, and $D_2 = -c/n_0 D_1^2 \beta_2$. Here c is the light velocity, n_0 is the refractive index intracavity, β_2 denotes the group velocity dispersion. When generating a frequency comb, the frequency of every comb line is $\omega_0 + D_1\mu$. This nature also determines the potential bandwidth of a frequency comb.

2.2 Generation approaches of microcombs.

As mentioned in introduction, microcombs are usually initialized by interplay between optical light field and optical microresonator. Based on the origin of generation, they can be divided into four main classes: microcomb based on nonlinearity, microcomb based on laser gain, microcomb based on electro-optic modulation, and microcomb based on multi-effect coupling.

Kerr frequency comb is one of the most widely studied type of microcombs since its invention in 2007 [9]. Due to the Kerr nonlinearity of microresonator, comb field can be established and enhanced via cavity-enhanced cascaded four-wave mixing (FWM) process, transferring the energy from pump field over broad spectrum band and even over octave spanning [13], as shown in the top panel of Fig. 3a. With pump laser tuning into microresonator resonance from blue-detuned side to build up the intracavity field, the comb field regularly evolves into primary combs or Turing pattern, chaotic state, and soliton state in turn [65] (bottom panel of Fig. 3a). Kerr soliton microcomb generation relies on the double balance of nonlinearity and dispersion, gain and loss in microresonators and the excitation of soliton microcomb should also overcome the thermal instability in microresonators. The nonlinear dynamics of a Kerr microcomb can be succinctly described by the well-known Lugiato-Lefever Equation (LLE) [66], which reads as

$$\begin{aligned} T_R\frac{\partial E(t,\tau)}{\partial t} =& [-\alpha - i\delta + iL\sum_{k\geq 2}\frac{\beta_k}{k!}(i\frac{\partial}{\partial\tau})^k \\ &+ i\gamma L|E|^2]E(t,\tau) + \sqrt{\theta}E_{in} \end{aligned} \tag{2}$$

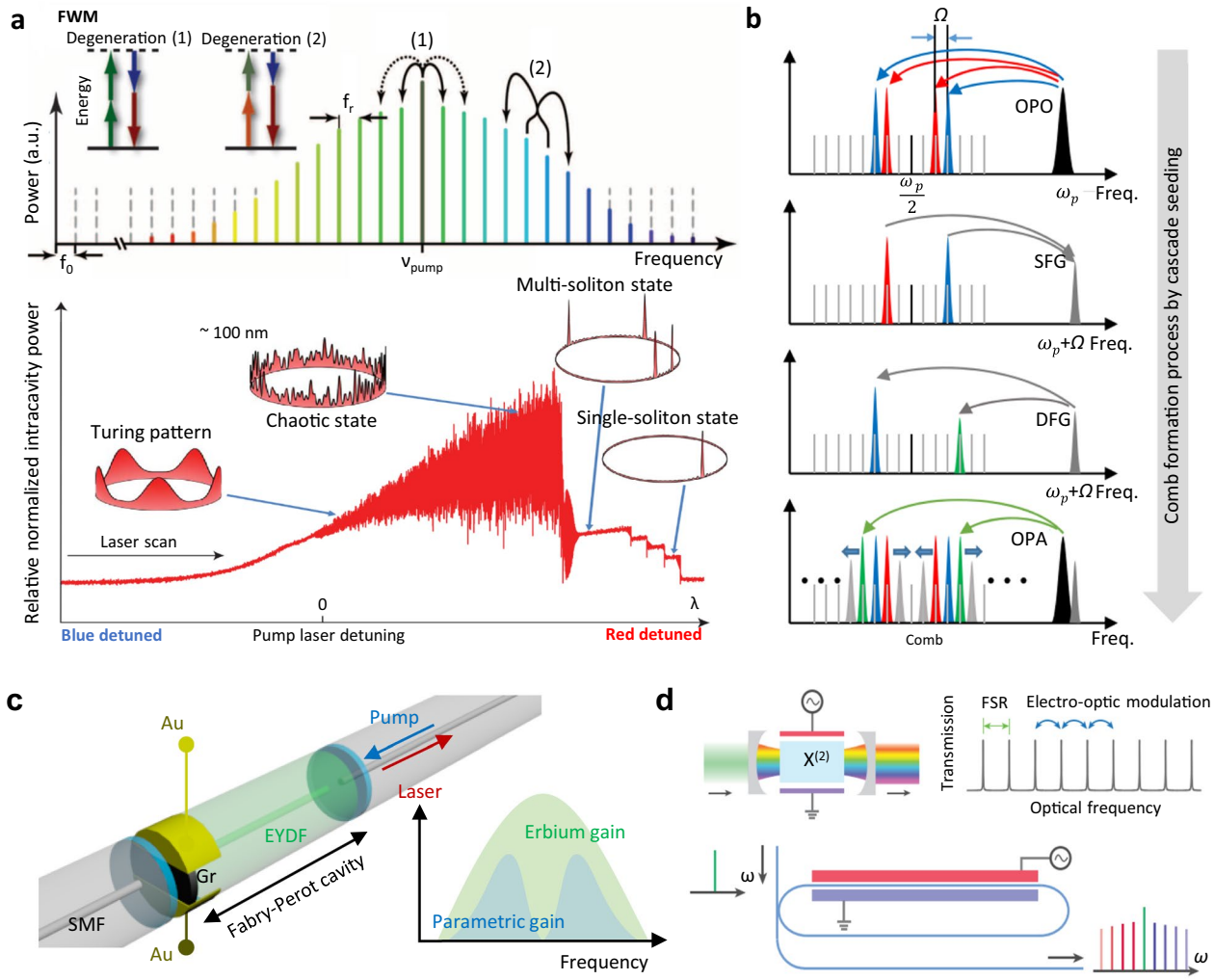

Fig. 3 Typical approaches for microcomb generation. **a**, Microcomb generation based on Kerr effect. Top panel: energy transfer process, bottom panel: intracavity power evolution including the Turing roll, chaotic state and soliton states [13, 65]. **b**, Microcomb generation leveraging the second order nonlinearity of material [72]. **c,** Microcomb generation in an active microcavity with laser gain [60]. **d,** Microcomb generation based on electro-optic (EO) modulator [77]

On the left side of this equation, t and τ describe the slow and the fast time, or the evolution time of the field envelope E and the time frame for temporal profile, respectively. T_R is the roundtrip time of light in the cavity. The right side can be divided into several terms, related to the loss per roundtrip α, the detuning δ, the dispersion β_k, the nonlinearity γ, and the driving term $\theta^{1/2}E_{in}$, respectively. In addition, L is cavity length, θ is the coupling coefficient and E_{in} is the field of driving pump. When thermal instability is augmented, the thermal-incorporated LLE can be further updated as [67–69]:

$$T_R\frac{\partial E(t,\tau)}{\partial t} = [-\alpha - i(\delta - \delta_{th}) + iL\sum_{k\geq 2}\frac{\beta_k}{k!}(i\frac{\partial}{\partial \tau})^k + i\gamma L|E|^2]E(t,\tau) + \sqrt{\theta}E_{in} \tag{3}$$

The thermal term δ_{th} can be expressed as

$$\frac{\partial \delta_{th}}{\partial t} = \frac{1}{C_p}\left[\alpha_T\frac{Q_L}{Q_{\text{int}}}P_{intra} - K\delta_{th}\right] \tag{4}$$

where C_p is thermal capacity of the cavity, α_T is the temperature coefficient of the detuning shift (1/℃), Q_L and Q_{int} are the loaded and intrinsic quality factors, respectively. P_{intra} shows the intracavity power, and K is the thermal conductivity. Nowadays, the thermal cooling technique has been successfully packaged with automated access to the soliton regime [70, 71].

Except for Kerr nonlinearity, the second order nonlinearity of material can also be used for comb generation, in a parametric down conversion or optical parametric oscillation process [72–74] (Fig. 3b). Even though the broadband phase matching can be a challenge, this is potentially a powerful method for comb generation in the band where high-performance pump laser is not easily accessible, such like mid-infrared (MIR), which is important for high resolution spectroscopy, sensing and ranging applications. Wang et al. [75] proposed and demonstrated a box resonator geometry fabricated over a MgO-doped lithium niobate wafer, enabling microcomb generation via $\chi^{(2)}$ optical parametric down conversion process, which can be described by the following mutually coupled three-wave equations

$$(\frac{\partial}{\partial z}+\beta_p\frac{\partial}{\partial t}+i\frac{\gamma_p}{2}\frac{\partial^2}{\partial t^2})E_p=-\alpha_pE_p+\frac{i\omega_p d_{eff}}{n_pc}E_sE_ie^{i\Delta kz} \tag{5}$$

$$(\frac{\partial}{\partial z}+\beta_s\frac{\partial}{\partial t}+i\frac{\gamma_s}{2}\frac{\partial^2}{\partial t^2})E_s=-\alpha_sE_s+\frac{i\omega_s d_{eff}}{n_sc}E_pE_i^*e^{-i\Delta kz} \tag{6}$$

$$(\frac{\partial}{\partial z}+\beta_i\frac{\partial}{\partial t}+i\frac{\gamma_i}{2}\frac{\partial^2}{\partial t^2})E_i=-\alpha_iE_i+\frac{i\omega_i d_{eff}}{n_ic}E_pE_s^*e^{-i\Delta kz} \tag{7}$$

Here subscripts p, s, and i denote the parameters of pump, signal, and idler, respectively. Then, z is the propagating distance, $\beta=1/v_g$ is the first-order dispersion, t is the propagation time, γ is the group velocity dispersion and E represents the optical field. On the right-hand side, α, d_{eff}, and n represent the propagation loss, effective nonlinear coefficient and refractive index of MgO-doped lithium niobate, respectively; ω is the angular frequency, c is the light speed and Δk denotes the phase mismatch. Relying on this nonlinear process, microcomb can be generated in 2 μm band, which has entered the boundary of MIR. Moreover, nonlinear dispersion control is possible with proper chirping to manipulate comb dynamics towards soliton comb generation thus higher coherence and stability. The comb state evolution generally obeys specific routine that can be stably accessed via conventional locking technology such like Pound-Drever-Hall (PDH) [76].

On the other hand, microresonator can be fabricated from materials with laser gain, enabling laser frequency comb in an integrated platform. Similar to its analog using bulk optics, the laser microcomb also acquires mode-locking components. By end-coating an electrically controllable graphene layer on the fiber resonator as a saturable absorber, Qin et al. [60] achieves low-noise mode-locked laser combs with tunable repetition rates (Fig. 3c). Different from conventional mode-locked laser, the laser microcomb features a repetition frequency at 10 s to 100 s GHz level due to the small size of microresonator. In addition, the development of integrated electro-optic (EO) modulator opens a different way for high-efficiency and controllable microcomb generation, known as EO microcomb [77] (Fig. 3d). The phase modulator can be directly assembled in microring resonators, enabling high-efficiency optics-microwave coupling [77, 78]. When the frequency of the driven microwave matches with the free spectral range of the microresonator, the cascaded sidebands originating from phase modulation, and the output field can be expresses as [79]:

$$E_{out}(t)=[\sqrt{(1-\alpha)(1-k)}-k\sqrt{\frac{1-\alpha}{1-k}}\frac{re^{-i\beta\sin\omega_m t}}{1-re^{-i\beta\sin\omega_m t}}]E_{in}(t) \tag{8}$$

where in α is insertion loss, k is coupling coefficient, and r is roundtrip electric filed transmission. β and ω denote modulation index and frequency of the phase modulator, respectively. When the driving beam E_{in} is a continuous wave, E_{out} formats a resonant EO microcomb. One of the major advantages of EO comb is that comb spacing can be defined and actively controlled by the frequency of the driven microwave.

Based on the above four mechanisms, diversified microcomb generation schemes are proposed [80], including fast frequency scanning [9, 30], filter-driven FWM [81], EO modulation [4, 82], power kicking [26], integrated [12, 83], forward and backward frequency tuning [84]. These approaches have been widely used for driving and generating microcombs, especially for the generation of soliton microcomb with high coherence and low noise characteristics. To meet practical application requirements, it is essential to sidestep intricate pump dynamics and the need for precise feedback stabilization when forming microcombs. Thus, the quest for simple, efficient, and deterministic methods to generate high-performance soliton microcombs has emerged as a critical area of focus in microcomb research. In this context, we will concentrate on exploring several innovative approaches.

In 2017, Guo et al. uncovered a universal dynamic and deterministic method for switching dissipative Kerr solitons in optical microresonators [84], as depicted in Fig. 4a. They discovered a straightforward mechanism that deterministically reduces the soliton count one at a time, uncovering effects uniquely linked to the soliton regime in both Si_3N_4 and MgF_2 materials. By harnessing this phenomenon, they experimentally demonstrated the multi-stability diagram of a microresonator. This technique enables the sequential decrease, monitoring, and stabilization of soliton states, particularly aiding in the feedback stabilization of single-soliton states. Building on

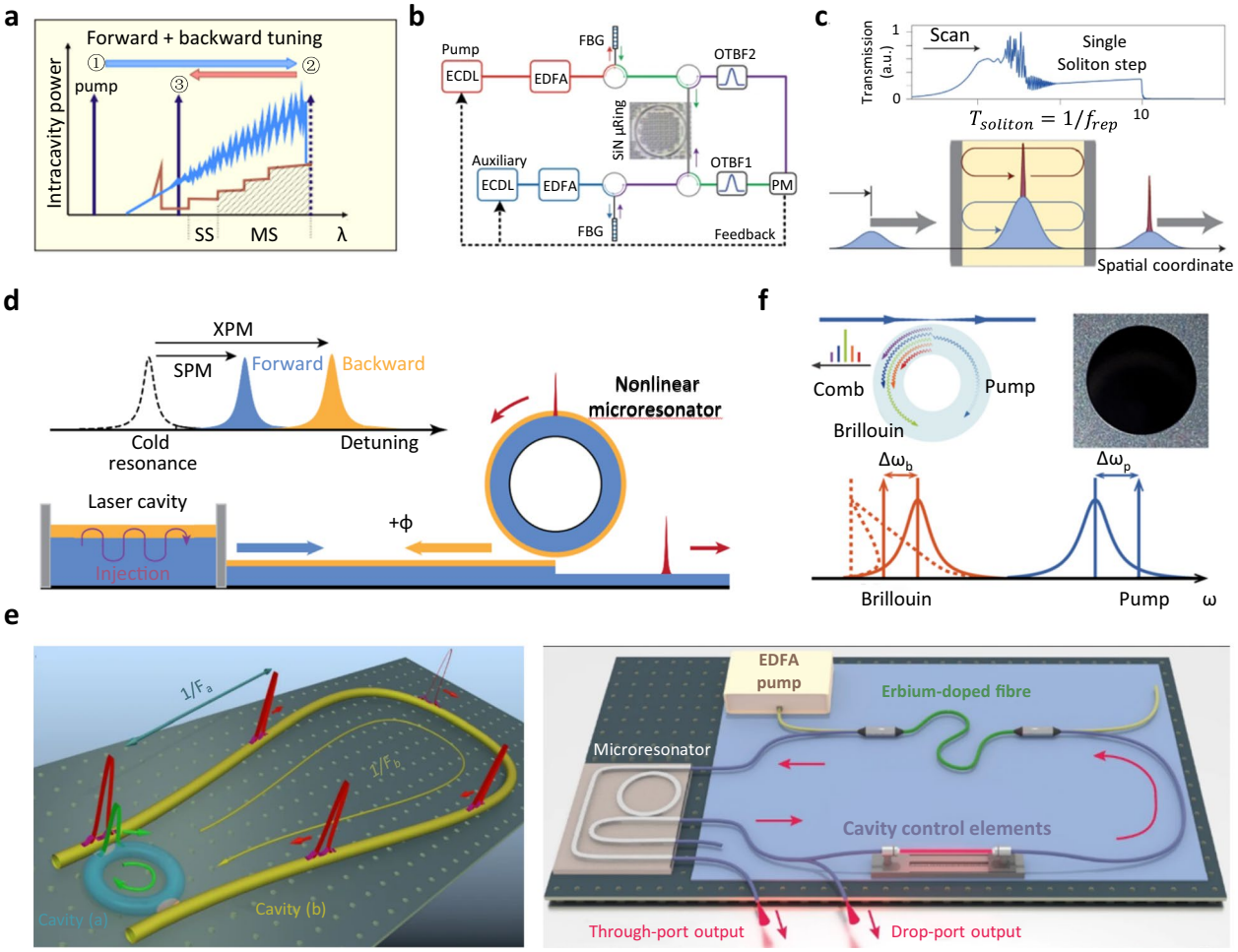

Fig. 4 State-of-art microcomb generation schemes in recent years. **a**, Backward frequency tuning [84]. **b,** Auxiliary laser assistance [67]. **c**, Pulsed pumping stretagy [85]. **d**, Turnkey operation [86]. **e**, Self-starting oscillation [88]. **f**, Two-step pumping method in hybrid cavities [92]

this work, Zhou et al. applied an auxiliary laser heating strategy to minimize thermal dragging dynamics that can occur during the formation of dissipative soliton combs [67], which can be theoretically characterized by two mutually coupled and thermal-incorporated LLEs

$$T_R\frac{\partial E_{comb}(t,\tau)}{\partial t} = [-\alpha - i(\delta_{pump} - \delta_{th}) + iL\sum_{k\geq 2}\frac{\beta_k}{k!}(i\frac{\partial}{\partial\tau})^k + i\gamma L(|E_{comb}|^2 + 2P_{aux})]E_{comb}(t,\tau) + \sqrt{\theta}E^{in}_{pump} \quad (9)$$

$$T_R\frac{\partial E_{aux}(t,\tau)}{\partial t} = [-\alpha - i(\delta_{aux} - \delta_{th}) + iL\sum_{k\geq 2}\frac{\beta_k}{k!}(i\frac{\partial}{\partial\tau})^k + i\gamma L(|E_{aux}|^2 + 2P_{comb})]E_{aux}(t,\tau) + \sqrt{\theta}E^{in}_{aux} \quad (10)$$

Here, Eq. (9) and Eq. (10) describe the field evolution of comb field E_{comb} and auxiliary laser field E_{aux}, respectively, and they can be regarded as expansions of **Eq.** (3), augmented with interplay between these two fields. This leads to the stable and robust generation of Kerr soliton singlets and soliton bursts, as shown in Fig. 4b. The process prevents sub-comb overlap at reduced pump powers and consistently yields nearly identical singlet soliton comb formations. It further reveals unexpected spontaneous soliton bursts when forming low-noise optical frequency combs out of continuum background noise. The auxiliary laser facilitates rapid synchronization of the pump laser with the cavity mode, thus providing a reliable means for soliton comb recovery and long-term stability,

even in the presence of strong external disruptions. In a pivotal study from 2017, Herr et al. presented their findings in Fig. 4c on the use of periodic picosecond optical pulses to pump a Fabry–Pérot microresonator, leading to the deterministic production of stable femtosecond dissipative cavity solitons atop resonantly enhanced driving pulses [85]. These microcomb solitons synchronize with the driving pulses, directly allowing all-optical manipulation of the soliton's repetition rate and adjustment of its carrier-envelope offset frequency. Offering advantages over continuous-wave-driven microresonators or nonresonant pulsed supercontinuum generation, their methodology is more effective, achieving broad bandwidth frequency combs with average driving power well below the parametric threshold of continuous-wave operation.

In an expanded framework, the generation of microcombs through multi-effect coupling in microresonators is emerging due to unprecedented physical mechanisms and the potential for exceptional turnkey performance. By connecting a laser diode and a microresonator in series, the latter can act effectively as a narrow-band filter to achieve injection-locking, thus purifying the output spectrum of the laser diode. More importantly, there exists a special operational regime that enables self-starting soliton comb formation [86, 87], see Fig. 4d. Additionally, turnkey operation has been observed in several other configurations, including fiber laser cavities that incorporate a microresonator, lithium niobate microrings that exhibit photorefractive effects, and so on [50, 88]. This turnkey operation is also achievable in laser soliton hybrid cavities [88–90]. The slow nonlinearities of a free-running microresonator-filtered fiber laser can transform temporal cavity solitons into the system's dominant attractor, leading to reliable, self-starting oscillation of microcavity solitons that are inherently robust to perturbations and capable of spontaneous recovery even after a complete disruption, as demonstrated in Fig. 4e.

Recently, schemes involving multiple nonlinearities have opened new avenues for microcomb generation. An intracavity Brillouin laser can serve as a secondary pump for Kerr comb excitation, while the primary pump maintains thermal stability of the cavity resonance, as illustrated in Fig. 4f. Such a Brillouin lasing often requires inter-mode phase matching [91]. Additionally, the linewidth narrowing effect of Brillouin lasing significantly reduces frequency noise from the primary pump by several orders of magnitude [92–94]. Furthermore, the Raman effect, another stimulated scattering phenomenon in microresonators, can contribute to Kerr comb formation through cross-phase modulation between the pump field and the Raman laser field [94, 95]. This enables simultaneous generation of combs across multiple spectral bands, uncovering new physics of comb formation and facilitating potential applications such as mid-infrared comb generation via difference frequency generation and precise spectroscopy for multi-species gas molecule detection. Moreover, by leveraging second-order nonlinearity, soliton microcombs can be extended even further, spanning wider wavebands up to an octave and enabling near-visible comb generation tied to precise molecular transitions [50, 96]. In the burgeoning lithium niobate on insulator (LNOI) platform, integrated modulation has become a more direct approach towards low-noise, highly efficient, and controllable comb states [50, 78].

2.3 Microcomb functionalizations and empowerments

The performance of soliton microcombs is extensively evaluated following soliton formation by examining the spectral width, pumping efficiency, and signal linewidth. A primary goal for advancing microcomb applications is to improve the performance capabilities of these devices. The spectral width of most soliton microcombs is generally restricted, primarily due to a balance between the gain bandwidth and chromatic dispersion.

First, numerous efforts have been directed toward extending the range of microcombs [97]. For example, Brasch et al. engineered the second and third order dispersion coefficients (β_2 and β_3) within a microresonator to achieve a fully coherent near-infrared optical frequency comb spanning from 2 to 3f (1300 nm to 2000 nm) [98]. Dispersive waves, such as Cherenkov radiation, were instrumental in this advancement, facilitating an extension of the coherent region, as depicted in Fig. 5a. This dispersion management strategy has also been employed effectively to merge sidebands [99]. In 2020, Zhang et al. demonstrated a method to expand the optical spectrum of a soliton microcomb produced in a microresonator [100]. This was achieved by using one laser operating at a wavelength within the anomalous dispersion regime of the microresonator to generate a bright soliton microcomb. Simultaneously, another laser in the normal dispersion regime helped to counteract the thermal effect on the microresonator and create a second frequency comb that was synchronized with the repetition rate. Its theoretical model is very similar to the aforementioned auxiliary laser heating strategy, which can be described in normalized form of LLEs

$$\begin{aligned}\frac{\partial \psi_p(t,\tau)}{\partial t} =&[-1-i\delta_p+i\sum_{k\geq 2}\frac{\beta_{p,k}}{k!}(i\frac{\partial}{\partial \tau})^k+i(|\psi_p|^2\\&+\sigma|\psi_a|^2)+\theta\frac{\partial}{\partial \tau}]\psi_p+F_p\end{aligned} \tag{11}$$

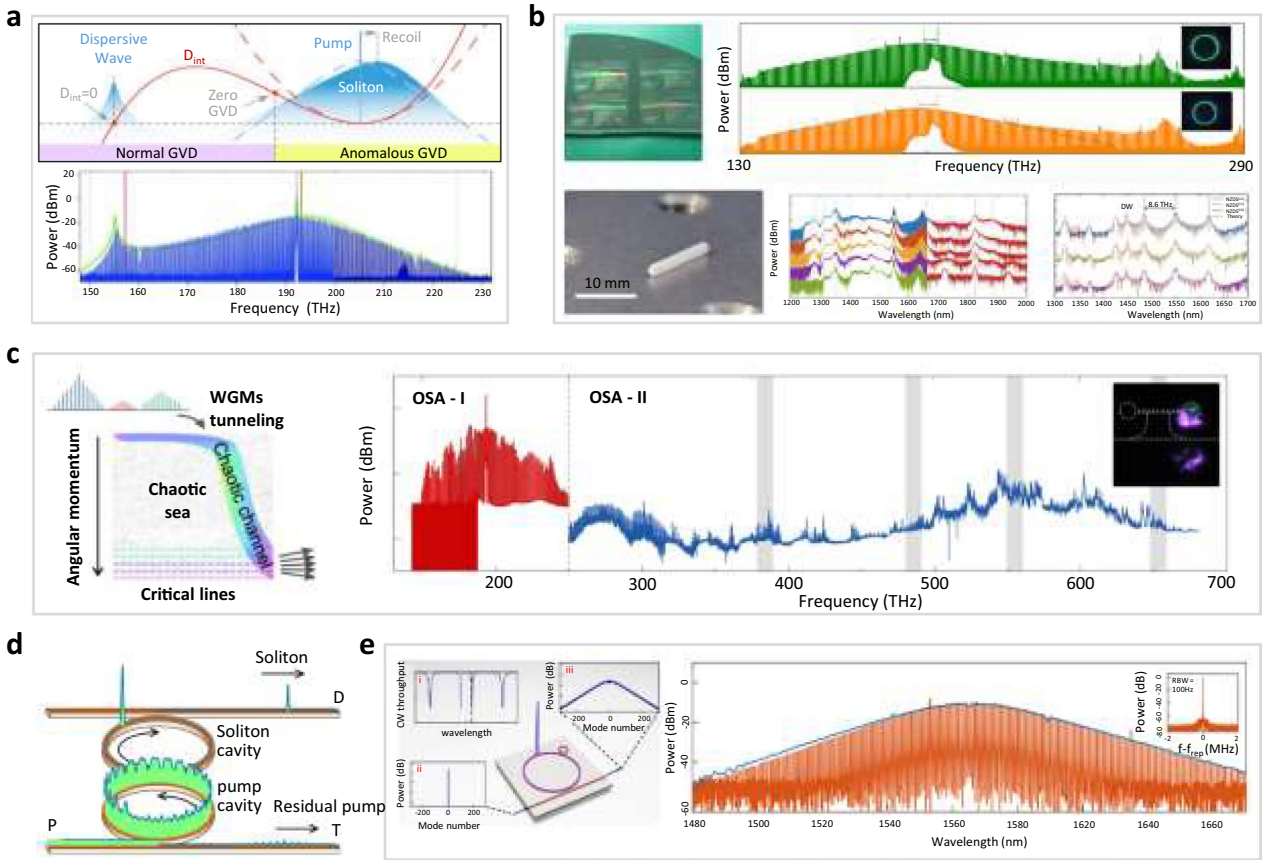

Fig. 5 Spectral broadening and efficiency enhancement for microcombs. **a**, Broadband Kerr soliton generation using Cherenkov radiation [98]. **b,** Wide span microcombs excited in dispersion engineered microcavities [102, 103]. **c,** Chaos assisted super-continuum microcomb [63]. **d,** High efficient soliton frequency comb driven by recycling pump energy [110]. **e,** Surpassing the nonlinear conversion efficiency of a soliton microcomb [112]

$$\frac{\partial \psi_a(t,\tau)}{\partial t} = [-1 - i\delta_a + i\sum_{k\geq 2}\frac{\beta_{a,k}}{k!}(i\frac{\partial}{\partial \tau})^k + i(|\psi_a|^2 + \sigma|\psi_p|^2) - \theta\frac{\partial}{\partial \tau}]\psi_a + F_a \tag{12}$$

Here subscripts p and a denote the parameters of primary and auxiliary pump lasers, respectively. θ represents the group velocity mismatch between primary and auxiliary pumping modes, and σ denotes the cross-phase modulation (XPM) coefficient, equaling to 2/3 for orthogonal polarization or 2 for parallel polarization. Such spectral broadening effects are also thoroughly investigated by considering the scattering of an externally injected probe wave from a dissipative cavity soliton circulating in a Kerr microresonator [101]. More recent developments by Wang et al., also based on dispersion engineering, led to the creation of a broadband soliton microcomb [102]. This design utilized two modes from different families with identical polarization that were nearly degenerate. A single-frequency laser served the dual purpose of both the pump wave and auxiliary wave, which resulted in an unprecedented long single-soliton step (10.4 GHz) and an octave-spanning bandwidth (1100–2300 nm). Additionally, Xiao et al. developed a fiber-based Fabry–Perot microresonator characterized by ultra-small anomalous group velocity dispersion, achieving 2/3-octave-spanning microcombs with more than 84 THz spanning and approximately 10 GHz spacing. These operated in the modulational instability (MI) state and, upon transitioning to the soliton state, presented a local repetition rate up to 8.6 THz and a span exceeding 32 THz, generating in excess of 3200 comb lines [103]. The outcomes of these two studies are illustrated in Fig. 5b. In addition, Moille et al. expanded the bandwidth

of a microcomb far beyond its anomalous dispersion region on both sides of its spectrum through spectral translation mediated by the mixing of a dissipative Kerr soliton and a secondary pump, achieving a soliton with a total bandwidth of 1.6 octaves (137–407 THz) [104].

Another strategy to enhance the bandwidth of microcombs involves combining parametric oscillation with other nonlinear effects, such as stimulated Raman scattering. Notably, the co-locking of Kerr and Stokes solitons—with approximately 100 nm spectral separation—has been excited in different geometries: a microdisk in 2016 and a microsphere in 2021. Due to their belonging to distinct transverse mode families, the Stokes and the Kerr soliton can trap each other [95, 105]. In 2018, Liu et al. demonstrated a broadband Kerr comb exhibiting spectral lines ranging from 145 to 275 THz and achieving a low parametric threshold of approximately 25 mW by employing a single-crystal aluminum nitride (AlN) microring [106]. Additionally, they observed a broadband Raman comb produced through Raman-assisted four-wave mixing. More recently, in 2022, Xia et al. successfully implemented cascaded Raman lasers and broadband Raman-Kerr combs (1400 nm to 1700 nm) within an integrated germanium antimony sulfide (GeSbS) microring [107]. Their studies focused on the effect of dispersion on the interaction between Kerr and Raman effects in chalcogenide glass microcavities. Apart from these two approaches, ultra-broadband microcombs can also be generated via chaos-assisted momentum transformation in optical microresonators [108]. Utilizing this mechanism, microcombs spanning more than two octaves (from 450 to 2008 nm) have been achieved, exploiting both $\chi^{(2)}$ and $\chi^{(3)}$ nonlinearities in a deformed silica microcavity [63], as illustrated in Fig. 5c.

Improving the efficiency and output power of a microcomb is another significant concern, particularly in communication applications where higher intrinsic soliton output power is required to minimize noise resulting from excessive amplification. Common phase-locked microcombs typically exhibit low conversion efficiency due to their dissipative soliton nature [26]. In 2017, Xue et al. made an experimental breakthrough by demonstrating coherent soliton microcombs with remarkably high conversion efficiencies, exceeding 30% in the fiber telecom band, achieved by applying dark-pulse mode-locking in the normal dispersion region [109]. Advancing this work, in 2019, Xue and colleagues introduced super-efficient temporal solitons within mutually coupled optical cavities [110]. Their innovative pump recycling strategy significantly enhanced power utilization efficiency, allowing for nearly complete pump recycling and surpassing the efficiency limitations of individual cavities, as illustrated in Fig. 5d. Similarly committed to enhancing efficiency, Cole et al. observed soliton crystals in monolithic Kerr microresonators, which offer higher conversion efficiency and output power than solitary solitons [111]. More recently, Helgason et al. addressed the fundamental efficiency limitation by inducing a controllable frequency shift in two linearly coupled anomalous-dispersion microresonators, targeting a specific cavity resonance and achieving conversion efficiencies over 50%, as depicted in Fig. 5e [112]. To further boost the output power of microcombs, recent proposals include driving soliton excitation with coherent pulses [113], enhancing conversion efficiency through photonic diatomic molecular structures [114], and compensating for intrinsic losses with intracavity erbium gain [115, 116]. These methods provide various pathways for improving the performance of Kerr microcombs.

In addition to efficiency or power improvements, managing the dynamic behavior of microcombs is a critical aspect of their development. Such control enhances the utility of microcombs in cutting-edge fields like data coding and signal processing. State-of-the-art techniques allow for manipulation of various parameters including intensity, frequency, repetition rate, and spectral range through electrical, mechanical, optical, and thermal methods.

Leveraging the Pockels effect observed in materials with second-order nonlinearity, it is possible to electrically adjust the intensities of individual comb teeth, facilitating spectral shaping [77, 117]. For instance, research by Zhang et al. showcased the ability to vary the oscillating frequency of a comb from 10 Hz to over 100 MHz using a dual radio frequency setup within a $LiNbO_3$ microresonator, as represented in Fig. 6a [77]. This approach is characterized by its significant electro-optical response, minimal optical attenuation, and the close integration of microwave and optical fields, allowing for dispersion manipulation. Using this method, the micro electro-optic (EO) comb can cover frequencies spanning beyond the full telecommunications L-band, achieving dispersion control across an octave range. A single device of this kind can produce over 900 comb teeth with a slope of 1 $dB{\cdot}nm^{-1}$ and a repetition rate of 10.453 GHz. Similarly, researchers have employed a $LiNbO_3$ microresonator to generate, select, and modulate a frequency comb on a unified monolithic chip [118]. They utilized a nanophotonic lithium-niobate platform notable for its pronounced electro-optic and Kerr nonlinearities coupled with low optical losses. By designing a high-Q lithium-niobate microresonator with engineered dispersion properties, they were able to create broad-spectrum Kerr frequency combs. Additionally, they isolated a single comb line using an electrically tunable add-drop filter

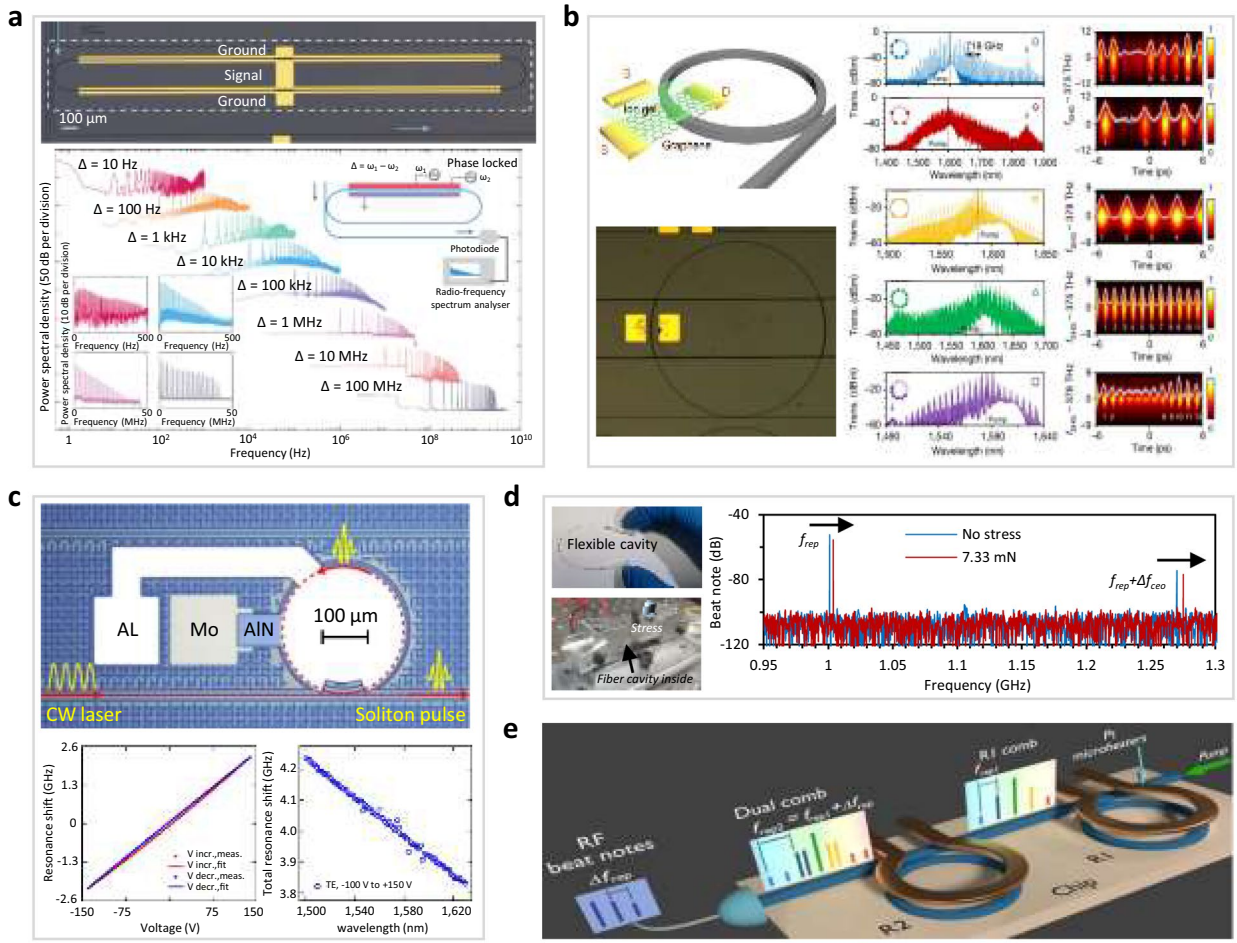

Fig. 6 Dynamic control of microcombs. **a**, Electrical tuning of microcombs in a $LiNbO_3$ microresonator [77]. **b,** Gate tunable Kerr soliton combs in a graphene deposited microring [59]. **c-d,** Mechanical tuning of a soliton frequency comb [44, 122]. **e,** Thermal control for soliton microcombs via integrated heater [83]

and modulated the intensity of that chosen line, integrating multiple functionalities within a single device.

Electrical control can program the dispersion and energy accumulation in a graphene based microcavity (Fig. 6b), enabling diverse soliton states and self-feedback stabilization [59, 60]. Specifically, by coupling the gate-tunable optical conductivity to a silicon nitride photonic microresonator, Yao et al. demonstrated the gated intracavity tunability of graphene-based optical frequency combs, thus modulating its second- and higher-order chromatic dispersions by altering the Fermi level. This produced charge-tunable primary comb lines from 2.3 terahertz to 7.2 terahertz, controllable coherent Kerr frequency combs, Cherenkov radiations and versatile soliton states, all in a single microcavity. In addition, the same group illustrated electrically controllable laser frequency combs in a heterogeneous graphene-fibre microcavity. By altering the Fermi level of atomically thick graphene, they simultaneously demonstrated the tunable absorption, controllable *Q*-factor, and fast optoelectronic feedback stabilization [119, 120]. Thus, this microcomb device can deliver tunable repetition rates, controllable wavelengths, and self-stabilized phase noise.

The emergence of piezoelectric materials, coupled with the refinement of integration processes, has made mechanical methods viable for manipulating microcombs. Voltage applied to a piezoelectric actuator can swiftly adjust the resonant frequency of a microcavity, offering improvements in linearity and modulation bandwidth (see Fig. 6c). A notable example is the integration of an AlN piezoelectric actuator onto an ultra-low loss Si_3N_4 photonic circuit, which enabled MHz-order bandwidth tuning [44]. More recent developments have seen tuning ranges exceed 1 GHz with impressively high ramping speeds up to 800 kHz, which have been successfully implemented in optical ranging applications [121].

Mechanical stress is another means to alter mode distribution in flexible fiber microcavities [92, 122]. Such manipulation has enabled the repetition offset of dual soliton microcombs to scan over a 2 MHz range, providing a mechanism for controlled photonic microwave generation (illustrated in Fig. 6d). Additionally, by injecting external light into the microcavity, controllable self-oscillation was found, leading to the synthesis of reconfigurable soliton crystals with order numbers ranging from 1 to 32 [123]. The stability of soliton can be optically tuned and enhanced by injecting another blue-detuned laser, relying on its opto-thermally induced cooling effect [124]. Besides, Dutt et al. observed that by using integrated microheaters, microcombs can be deterministically tuned into soliton mode-locked states [83], as depicted in Fig. 6e. Zhu et al. employed an auxiliary laser to achieve tunable line-to-line wavelengths across 0.8 nm for Kerr combs and 2.67 nm for Raman-Kerr combs [125]. Further advancements in 2021 by Tan et al. utilized similar laser-assisted technology to realize bi-directional on–off switching of dual Kerr soliton microcombs within a single whispering-gallery-mode (WGM) resonator [116].

3 Microcomb based information carriers

A distinctive characteristic of the microcomb is its central frequency situated within the optical spectrum, with a repetition rate that falls within the radio frequency range. This inherent advantage positions it as an effective information carrier, seamlessly connecting the realms of photonics and electronics. This section is dedicated to exploring applications of the microcomb, including signal generation and synchronization, telecommunications, and quantum information.

3.1 Signal generation & synchronization

The generation of stable electromagnetic wave oscillation across a spectrum from millimeter waves to optical frequencies is critically important for contemporary science and technology. It supports an array of frontier applications spanning from communication to metrology that are integral to our society. The leading-edge techniques currently employed for generating tunable continuous-wave (CW) radiation encompass electronic technologies [126], frequency multiplication [127], photomixing with dual infrared wavelengths [128], quantum-cascade lasers (QCLs) [129], molecular gas lasers [130], free-electron lasers [131], and CMOS-compatible photonic integrated technologies [132]. Traditional electrical-circuit methods encounter limitations with respect to the operable frequency range and phase noise performance. While frequency multiplication can provide milliwatt-level radiation power, it typically struggles to exceed 1 THz in frequency. Furthermore, the operational frequency range of these methods is often restricted due to challenges like impedance matching and waveguide cutoff constraints.

Photonic technology is revolutionizing the generation of reliable high-frequency continuous-wave (CW) radiations [133]. Through direct heterodyne photo-mixing, it is possible to produce millimeter or terahertz radiations with a flexible frequency tuning range and a wide operating frequency bandwidth. Recent advances have led to the generation of high-power and coherent millimeter waves, achieved by integrating microresonators with optical frequency division (OFD) techniques, rapid direct detection methods, and optical spectral shaping technologies [134, 135]. The spectral purity of the signals generated has been exemplified in Fig. 7a [136]. To address the challenges posed by direct millimeter wave photodetection, including issues of spectral purity and stability, a variety of innovative optical technologies have been explored. These include W-band optoelectronic oscillators [137], electro-optic (EO) frequency division methods [138], high-Q microresonator oscillators [139], and advancements in OFD [140, 141]. The OFD technique, in particular, was originally developed for ultra-low noise microwave generation, employing optical clock methodologies and femtosecond-laser-based broadband self-referenced frequency combs. This approach has led to unprecedented noise performance levels.

Frequency division can be succinctly represented as $f_{\mathrm{rep}}=(\nu_0\text{-}f_{\mathrm{ceo}})/n$, where ν_0 and f_{ceo} denote the reference frequencies within the optical and microwave realms respectively, and n is the integer multiple that defines the frequency division. The soliton microcomb functions as a high-frequency mechanism when used in conjunction with ultrafast optoelectronic devices, thus facilitating OFD in both the millimeter-wave and terahertz-wave domains through analogous operational principles. One of the primary challenges in this field is the stable and accurate attainment of conventional self-referenced frequency combs, which poses obstacles in the process of frequency doubling.

To circumvent these difficulties, the method of externally locking two comb teeth has emerged as a viable alternative, albeit at the cost of a reduced frequency division ratio. This approach can involve the utilization of two low noise Brillouin Stokes waves [134, 142], external-cavity stabilized lasers [143], among other techniques. A process of generating divided millimeter-wave frequencies is depicted in Fig. 7b. Furthermore, the utilization of Kerr nonlinearity within microresonators has recently enabled the passive, electronics-free phase locking of a frequency microcomb to an injected reference laser, a development relevant to optical clockwork synthesizers [144]. The experimental demonstration corroborates the anticipated frequency division behavior. For the

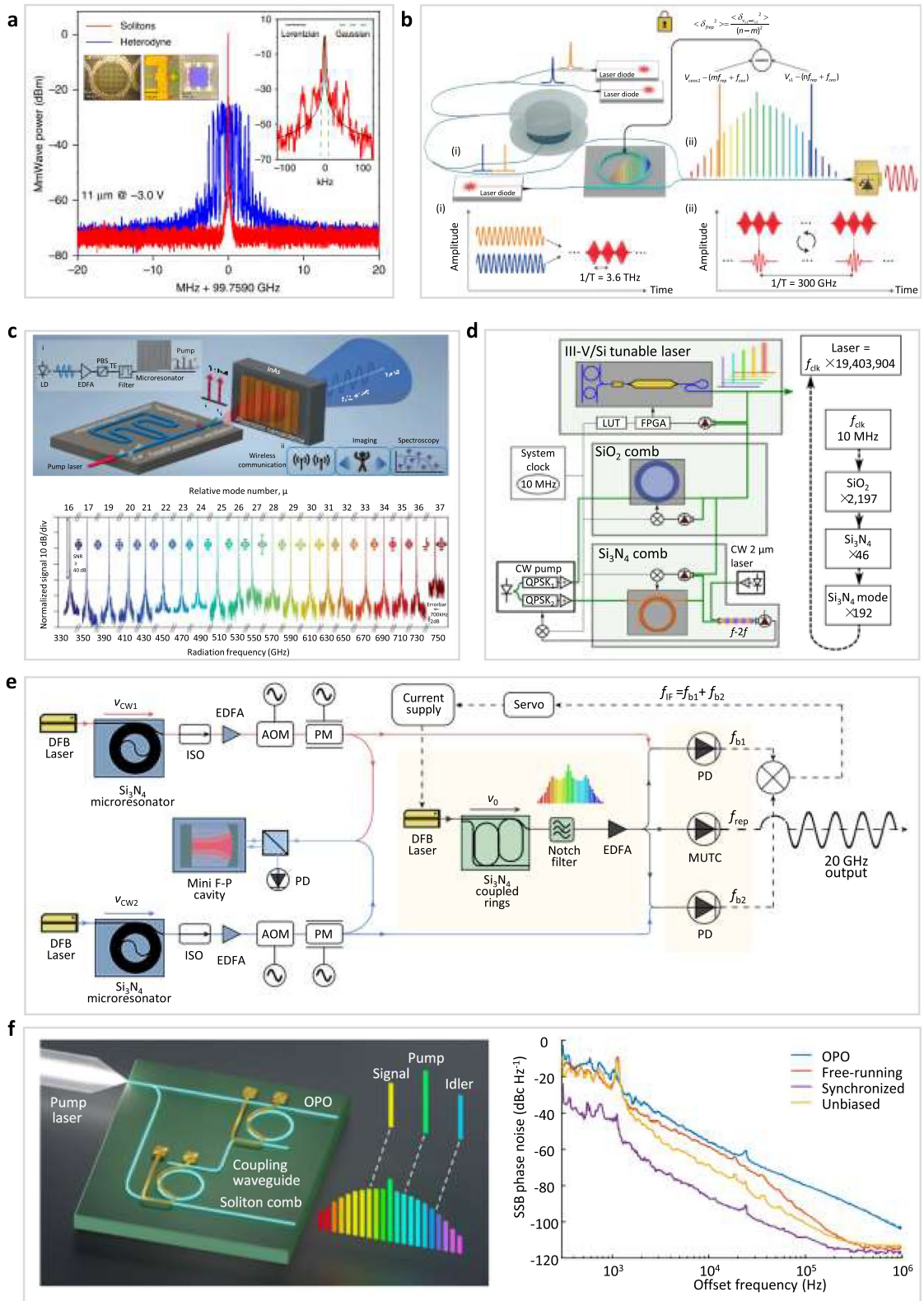

Fig. 7 Low noise millimeter-terahertz wave generation and optical frequency synthesis. **a**, High-power millimeter wave generation [136]. **b,** Millimeter wave frequency division signal generation [134]. **c**, Optical-to-terahertz down-conversion using a plasmonic nanoantenna array and chip-scale optical parametric oscillation [145]. **d,** Chip-scale optical frequency synthesizer [33]. **e,** Photonic chip-based low-noise microwave oscillator [154]. **f,** On-chip low-noise microwave generation via frequency division [156]

generation of signals in the terahertz domain, researchers have resorted to photomixing methods. Coherent terahertz radiation has been successfully produced by converting optical frequencies down to the terahertz range. This conversion is achieved by employing a plasmonic nanoantenna array in tandem with chip-scale optical parametric oscillation, with the methodology illustrated in Fig. 7c [145].

To generate stable optical frequencies, various methods are employed, such as semiconductor lasers with external cavity techniques [146, 147], stabilization of optical frequencies via optical transitions [5], and optical frequency synthesis [148]. Both the external-cavity technique and optical transition stabilization face challenges related to tunability and precision limitations. Optical frequency synthesis, which is revolutionizing ultrafast science and metrology, takes its origin from conventional synthesizer techniques that synthesize radio and microwave-frequency signals for use in communication and radar navigation systems. Over recent decades, optical synthesizers have been demonstrated using table-top mode-locked laser frequency combs and photonic-crystal fiber-based supercontinuum generation to achieve absolute frequency control. However, these solutions have been confined to laboratory settings due to their size, power consumption, and cost constraints. The synthesis of absolute frequency in the optical domain can be formulated as $\nu_n = nf_{rep} + f_{ceo}$, where f_{rep} and f_{ceo} are microwave frequencies, and n is an integer representing the frequency multiplication factor. With substantial advances in integrated optics, highlighted by the successful creation of a phase-locked microwave-to-optical link [149] and high-efficiency waveguides [150], optical frequency synthesis is poised for new stages of broader application.

Leveraging microcombs, a low relative uncertainty chip-scale optical frequency synthesizer is achieved via phase-locking both a comb line and the intrinsic comb spacing [151]. This advancement harnesses the power of heterogeneously integrated III-V/silicon tunable lasers, nonlinear on-chip frequency combs, and highly efficient nonlinear waveguides. Such integration allows for user-defined programmable optical frequencies, easily controlled through the manipulation of external reference clocks, as illustrated in Fig. 7d [33]. Crucial to this setup are the phase stabilization of an interlocked soliton microcomb pair at microwave and terahertz frequencies, as well as precise dispersion management that affects the spectral profile. With the incorporation of fully integrated silicon-based tunable lasers, an optical frequency synthesizer is constructed that self-calibrates through adjustments to the repetition rate of its internal mode-locked laser, benefitting from advancements in silicon photonics and rare-earth-doping techniques [152]. Further confirmations of such a system's capabilities are exemplified by incorporating a supercontinuum waveguide and a second harmonic generator within a silicon photonics platform [153]. Moreover, remarkable methods are demonstrated recently for integrated optical-frequency-division based on dual-mode locking [154] and chip-scale optical parametric oscillation [155, 156], which are promising for the high-purity millimeter and terahertz emission, as Fig. 7e, f shows.

Furthermore, heterogeneous integration enables the production of high spectral purity signals at millimeter, terahertz, and optical wavelengths in form factors that are compact, cost-effective, and suited for high-volume manufacturing. By combining active and passive components—semiconductor lasers and amplifiers, photodetectors, electro-optic modulators, passive waveguides, and CMOS electronics—all on a single silicon chip, these agile oscillation sources are redefining potential applications. The availability of these technologies marks the dawn of a new era, laying a versatile foundation that holds promise for advancing fields from space science to life sciences.

3.2 Data delivery

Data transmission relying on optical technologies underpins modern information systems. Optical communication, which serves as the backbone of these systems, leverages various physical channels such as optical fiber [157] and free-space atmospheric links [158] to revolutionize traditional communications. Utilizing highly parallel techniques like wavelength division multiplexing (WDM) [159], polarization multiplexing, and spatial-mode division multiplexing [160], along with spectrally efficient advanced modulation formats [161], allows for data transmission capacities exceeding several petabits per second. The advent of silicon photonics platforms facilitates the integration of photonic–electronic devices, including lasers, modulators, detectors, and microrings-based WDM, through large-scale, fabless CMOS processing, advancing towards chip-scale terabit-per-second transceivers. Chip-scale data transmitters with distributed feedback (DFB) laser arrays [162] have been successfully developed on indium phosphide (InP) substrates. These offer a substantial number of channels, although incorporating with other silicon photonic components presents challenges due to material interfaces. Additionally, the number of channels and wavelength stability are limited by the gain bandwidth of semiconductor materials and thermal effects. Besides, key parameters such as data speed, spectral and energy efficiency, integration footprint, and data capacity are crucial. Intensifying research efforts to integrate these components and

minimize the footprint is an important direction for further development.

Microcombs offer a viable alternative to traditional laser arrays for wavelength division multiplexing (WDM), particularly in scenarios that demand significant scalability to meet the burgeoning demands of internet communications. With their inherently low phase and amplitude noise paired with an adequate number of carrier channels, microcombs are poised to transform terabit communication systems. They enable transmission techniques such as orthogonal frequency-division multiplexing (OFDM) [163] and Nyquist-WDM [164], which use tightly packed subcarriers. Benefiting from less random wavelength drift, microcombs provide a precise broadband wavelength grid, minimizing crosstalk between neighboring data channels and reducing the need for protective guard bands. The phase coherence between channels also facilitates joint digital signal processing across multiple data channels, leading to reduced power consumption and circuit complexity. Explorations into microcomb-based data transmission include experiments using spectrally broadened mode-locked femtosecond pulses and the external modulation of continuous-wave lasers [165, 166]. Through multi-stage four-wave mixing (FWM) processes within Kerr-nonlinear microresonators, high-power, large-spacing Kerr frequency combs have emerged as promising tools for handling vast volumes of data transmission. These systems also offer the advantages of dispersion-tailored parametric conversion over traditional gain emission in active media, with the added benefit of flexible and scalable modulation depth and channel bandwidth.

Data transmission at gigabit-per-second rate has been achieved utilizing a Kerr microcomb combined with quadrature phase-shift keying and 16-state quadrature amplitude modulation techniques [20]. Upon integrating feedback stabilization, the data transmission rates exceeded one terabit per second. Further advancements involved the use of two interleaved dissipative Kerr soliton (DKS) frequency combs, which facilitated tens-of-terabits-per-second data stream across the full range of telecommunication C + L bands, coupled with local oscillation detection [167]. Additional methods were developed to establish chip-scale data transceivers employing coherence cloned Kerr soliton microcombs through dual-point locking mechanisms [168], wavelength- and mode- multiplexing via photonics inverse-design on silicon photonic circuits [169], dark-pulse comb configurations [170, 171], and spatial multiplexing techniques [172]. These were used alongside phase-correlated channel data demodulation for improved performance. Additionally, a terabit optical orthogonal OFDM superchannel exhibited high spectral efficiency [173]. Ultra-dense optical data transmission and ultrafast optical circuit switching were also successfully carried out over standard fiber and arrayed waveguide grating respectively using a singular frequency comb chip source [174, 175]. The amalgamation of diverse photonic integration platforms, including III–V semiconductors [176], ring resonators equipped with low-loss Si_3N_4 technology [177], as well as compact and energy-efficient multiplexing and de-multiplexing filters based on large-scale silicon photonic integration [178], has played a pivotal role. Furthermore, thin-film lithium niobate modulators and III–V uni-traveling-carrier photodetectors have contributed to these developments [179, 180]. Collectively, these innovations are paving the way toward chip-scale petabit-per-second transceivers.

The Kerr microcomb has proved to be a versatile tool, enhancing the performance of fiber-based large-capacity communication systems, as well as applications in free-space and wireless communication domains, as depicted in Fig. 8a [20, 181]. By combining two frequency microcombs spectrally, a groundbreaking data transmission rate of 50 Tbit/s was achieved using 179 distinct optical carriers, illustrated in Fig. 8b. This setup enabled error-free, multi-channel coherent data transmission over a 75 km fiber link [167]. Subsequently, leveraging dark-pulse microcombs led to improved data transmission quality, thanks to the higher optical signal-to-noise ratio afforded by increased single comb line power, as shown in Fig. 8c [171]. Building on these advances, terabit-scale coherent data transmission has been explored using coherent cloned soliton microcombs. This method involved pump laser propagation and the application of two-point locking techniques, detailed in Fig. 8d [168]. For instance, a remarkable feat in ultra-dense optical data transmission reaches a line rate of 44.2 TB/s and a spectral efficiency of 10.4 bits/s/Hz during a field trial over an existing network infrastructure. In this work, bit error rate, spectral efficiency, and generalized mutual information (GMI) across the C-band are summarized in Fig. 8e [174]. Besides, Oxenlowe et al. successfully demonstrated data transmission capability at 1.84 PB/s over a 37-core, 7.9 km long multi-core fiber utilizing 223 wavelength channels, as documented in Fig. 8f. Projections for systems with the potential to reach capacities up to 100 PB/s were also discussed, employing highly parallel space and wavelength multiplexing techniques [170]. In addition to capacity testing, key technical parameters have been thoroughly investigated. These include modulated optical spectra, signal-to-noise ratio (SNR) metrics, constellation mappings, eye diagrams, SNR, and bit-error-rate (BER) estimations across multiple channels considering the forward error correction (FEC) threshold, as well as the analysis of BER sensitivity performance.

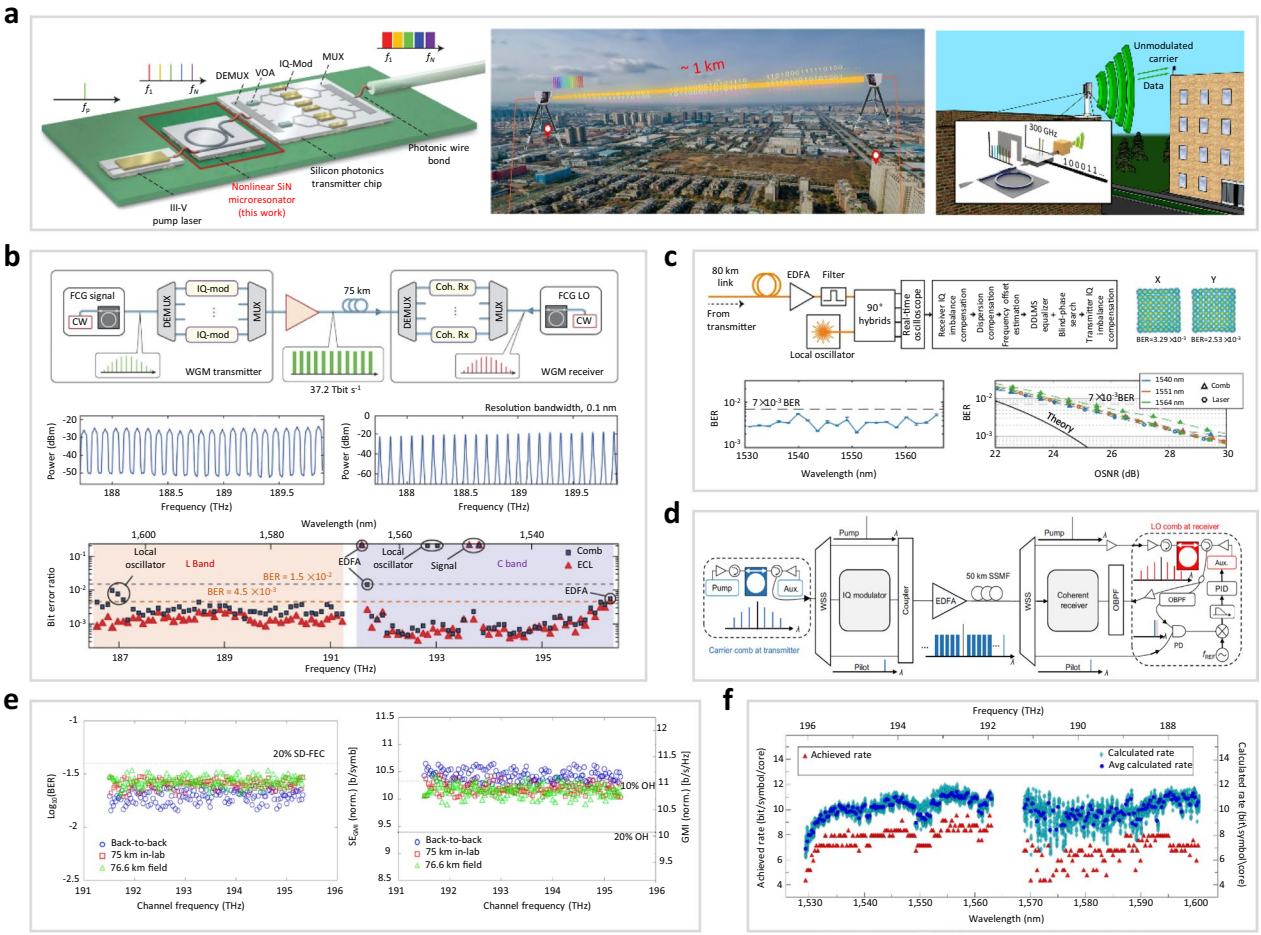

Fig. 8 Missive parallel data transmission based on microcombs. **a**, Three communication scenarios: Fiber coherent communication [20], Long-distance free-space communication [136], and Wireless communication [181]. **b,** Dual microcomb based data transmission [167]. **c,** Dark-pulse microcomb based data transmission [171]. **d,** Coherence-cloned data transmission [168]. **e–f,** Ultra-large capacity and Petabit data transmissions [170, 174]

3.3 Quantum information carriers

Cavity-enhanced devices such as microcombs are also deeply investigated and widely attractive in quantum information technology, thanks to the high *Q*-factor, small mode volume, and flexible dispersion engineering, which allows strong interaction between photons and other quantum systems. For instance, the quantum light generation, hyperentanglement harnessing and the quantum transduction have been demonstrated in recent years in optical cavities [182–185]. These advancements highlight the significance of cavity-enhanced devices and have great potential for the development of practical information technologies exploiting effects of quantum physics. In particular, optical microcombs are capable of providing hundreds of quantum channels from a single microresonator and represent a new generation of non-classical light sources for realizing compact and large-scale quantum optical systems with applications in quantum communications, quantum computing and quantum metrology [186–188].

The quantum counterpart of the classical frequency combs, known as "quantum frequency combs", exhibits multi-modal properties and can achieve photon entanglement in discrete frequency modes. This makes quantum frequency combs a significant candidate for generating multi-wavelength quantum entanglement. With the second order ($\chi^{(2)}$) and the third order ($\chi^{(3)}$) nonlinear optical materials, integrated quantum light sources have been achieved based on the processes of spontaneous parametric down-conversion (SPDC) and spontaneous four-wave mixing (SFWM) [189]. In 2014, Reimer et al. generated the generation of five correlated photon pairs based on Hydex platform [190]. As shown in Fig. 9a, they experimentally achieved the generation of multiphoton entangled quantum by means of integrated frequency combs with Hydex in 2016, showing attractive

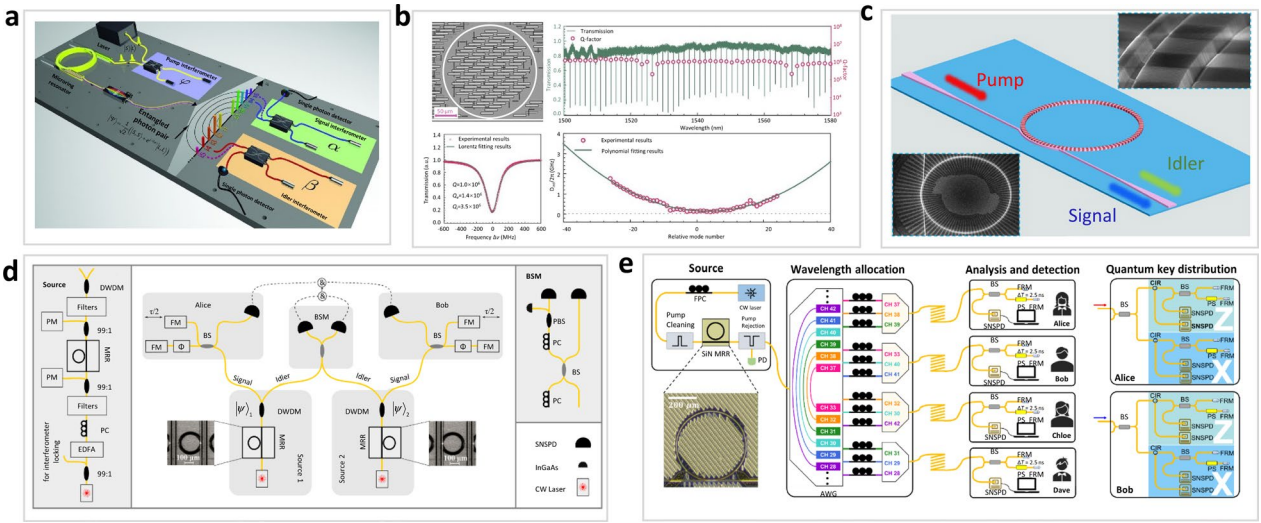

Fig. 9 Microresonator and microcomb based quantum information. **a**, Generation of multiphoton entangled quantum states with Hydex microring resonator [191]. **b**, Generation of multi-wavelength quantum photon pairs with silicon nitride microring resonator [194]. **c**, Generation of ultrabright quantum photon source using lithium niobate microresonator on chip [198]. **d**, Entanglement swapping between independent and asynchronous integrated photon-pair sources with two silicon nitride microring resonators [206]. **e,** Four-user entanglement-based quantum key distribution with silicon nitride microring resonator [207]

properties such as high scalability through multiple mode operation, high purity of generated entangled photons, and high compatibility with fiber optic technologies [191]. Furthermore, in 2017, scientists achieved the generation and coherent manipulation of high-dimensional quantum entangled states [192]. Using a silicon nitride microring with a Q-factor of 2×10^6, the generation of correlated photon pairs was realized, where the single-side counting rate of detected signal/idler photon reaches 290 kHz when the pump power is 3 mW. With a silicon nitride microring resonator of a free spectral range of ~ 40 GHz, Lu et al. realized the generation of 51 photon pairs and reconstructed the full density matrix in up to an 8×8-dimensional two-qudit Hilbert space [193]. More recently, Fan et al. [194] reported the multi-wavelength quantum light source on silicon nitride microring with a free spectral range of 200 GHz. The generation of eight-wavelength-paired photon pairs were realized in a wavelength range of 25.6 nm. With device optimization and noise rejection, this source enabled the generation of energy-time entanglement with a visibility of $99.39\pm0.45\%$ (Fig. 9b).

As a widely used optical material, lithium niobate has a high second-order nonlinear coefficient, which can be used to generate high-quality correlation/entangled photon pairs [195–197]. As shown in Fig. 9c, based on periodically poled lithium niobate microring, Ma et al. [198] realized high-quality photon pair generation with coincidence-to-accidental ratio, i.e., CAR, up to 14,682 and heralded single-photon autocorrelation. Xue et al. realized photon-pair generation rate of 2.79×10^{11} Hz/mW in 160-nm SPDC bandwidth based on a lithium niobate on isolator chip, eight-channel multiplexed energy-time entanglement was demonstrated by measuring the Franson interference with visibilities of over 97% [199]. Besides, in 2022, Guidry et al. [200] reported that a stable temporal lattice of solitons can isolate a multimode below-threshold Gaussian state from any admixture of coherent light, and predict that all-to-all entanglement can be realized for the state. In 2023, Ma et al. demonstrated the entangled photon pair generation in an integrated silicon carbide platform for the first time with the two-photon interference fringes exhibiting a visibility larger than 99% [201]. In addition to generating single/entangled photons, microcombs can also be used to generate squeezed light [202, 203]. In 2018, Stern et al. demonstrated a battery-operated integrated frequency comb generator, exciting low-noise soliton microcombs using only 98 milliwatts of electrical pump power [204]. In 2019, Raja et al. showcased an electrically-driven soliton microcomb by coupling an indium phosphide laser diode chip to a high Q Si_3N_4 microcavity [205]. These achievements provide powerful tools for generating entangled photons or squeezed light, offering more convenient operation and lower power consumption.

With the development of quantum frequency combs, entangled photon sources based on microcomb technology also have been extensively studied in quantum key distribution and quantum swapping benefitted to the natural property of multi wavelength of the resonator.

In 2021, Samara et al. [206] achieved the entanglement swapping between independent and asynchronous integrated photon-pair sources using two silicon nitride microring resonators, as shown in Fig. 9d. The interference visibility is over 91%, which shows the great potential of integrated devices for distributed quantum network architectures and protocols. Furthermore, to realize a large-scale quantum network, it is quite important to establish communication links among multiple users with integrated multiwavelength quantum light sources. In 2022, Wen et al. [207] experimentally demonstrated a fully connected four-user quantum network with the generated comb-like bipartite energy-time entangled states in a silicon nitride microring resonator, paving the way for the development of large-scale entanglement-based quantum network, which is illustrated in Fig. 9e.

4 Microcomb based information acquisition

Frequency combs are widely acknowledged for their inherent stability, positioning them as essential "rulers" in metrology and high-precision detection applications. The implementation of frequency combs has substantially enhanced resolution across various measurement systems. Microcombs, notable for their compact size, adaptable design, and customizable features, stand out as particularly suitable for rapid and precise information gathering. In this section, we will explore the advancements facilitated by microcomb technology in the fields of spectroscopy, LiDAR, and sensing.

4.1 Microcomb based spectroscopy

Rapid and precise characterization of optical and vibrational spectra in cluttered environments has the potential to identify species and provide early alerts. The use of multiphoton interactions between light and atoms to probe these elements, particularly for detecting trace gases, is proving beneficial. Spectroscopy, which spans the ultraviolet to terahertz spectral range, is capable of analyzing a mixture of analytes amidst both inhomogeneous and homogeneous broadening [208, 209]. Critical parameters for laser spectroscopy encompass tunability of the center wavelength, frequency agility, total optical power, signal-to-noise ratio (SNR), sensitivity, precision, spectral resolution, system footprint, measurement times, and acquisition rates. A fast acquisition rate is crucial for the study of instantaneous dynamics but must be balanced against spectral resolution. Additionally, the SNR diminishes as the number of sampling spectral components increases for a given incident optical power on photodetector. Advanced laser spectroscopy techniques leverage nonlinear supercontinuum photonics, microwave photonics, ultrafast optics, and quantum optics. The electro-optic intensity modulators, mode-locked femtosecond lasers, and continuous-wave lasers with narrow linewidths, all featuring complex synchronization, serve as laser sources for fundamental spectroscopy. Mid-infrared combs are generated using difference-frequency-generation, optical parametric oscillation, or supercontinuum generation with mode-locked femtosecond lasers, as well as electro-optic frequency combs with varying repetition rates. This multidimensional and sensitive approach to laser spectroscopy facilitates diagnostics of non-static phenomena in liquid or condensed matter and contributes to atmospheric monitoring efforts.

Dual-frequency-comb spectroscopy (DCS) employs two combs with slightly divergent repetition rates; one comb traverses a test sample while the other serves as a reference, circumventing the need for bulky mechanical spectrometers [210, 211]. The architecture's output is captured by a high-speed photodetector, producing a periodically fluctuating interferogram. This data is then subjected to Fourier transformation to extract the spectral information. Recent advancements have led to the development of spectroscopy devices integrated onto chips, enabling real-time identification of trace molecules for gas sensing. These on-chip devices achieve rapid acquisition rates and exceptionally high signal-to-noise ratios. Scientists employ microcombs in spectroscopy due to their compact size, high coherence, and the potential for integration with on-chip or in-module technologies. The microresonator's ability to enhance light-matter interactions in a small volume, due to its high Q factor, facilitates the detection of minute spectral features, thus allowing for the detection of trace amounts of substances. Additionally, related to conventional frequency combs based on mode locked lasers, microcombs offer faster acquisition times and can be fabricated with compatible materials for different spectral regions, making them versatile tools for a variety of sensing applications ranging from environmental monitoring to medical diagnostics. In addition, due to their high repetition frequency, it is easier to achieve ultra-broadband coverage in a microresonator. The microcombs' compatibility with established semiconductor fabrication techniques also presents a path toward scalable and cost-effective production, further enhancing their appeal.

Figure 10a illustrates a miniaturized, soliton microcomb-based dual-microresonator DCS chip. This platform integrates a directional coupler to delineate the gas cell spectral absorber [212]. The figure also presents measured molecular absorption spectra for comparison with those obtained using a wavelength-calibrated scanning laser system. In Fig. 10b, we show

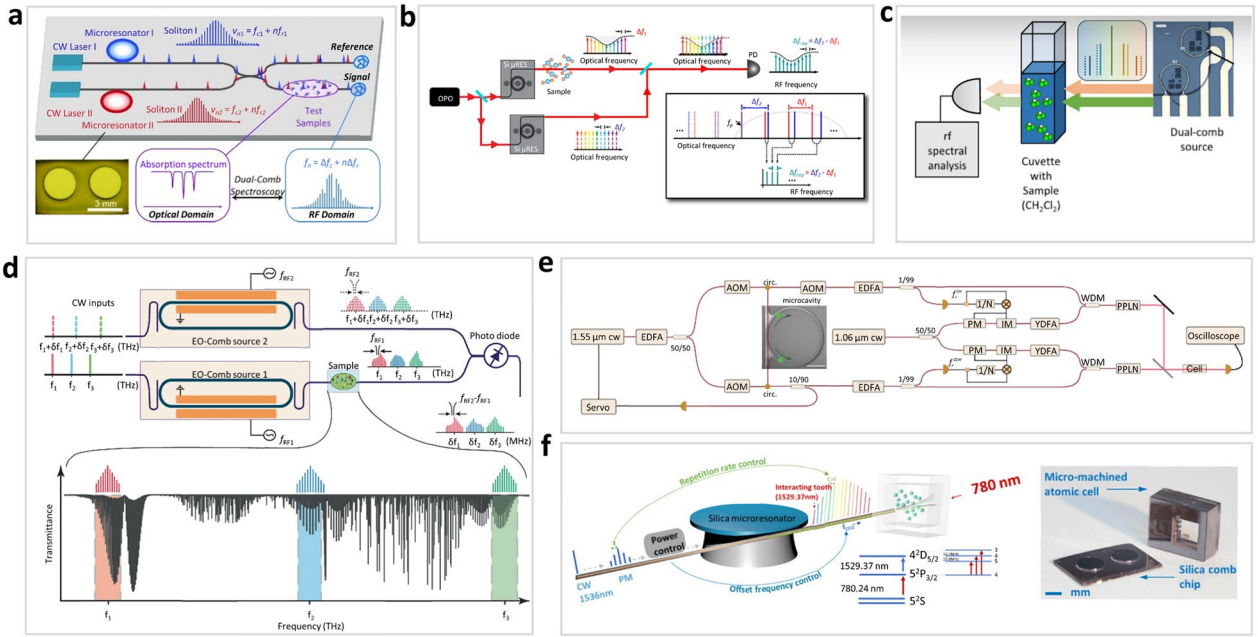

Fig. 10 Microcomb based spectroscopy. **a**, Microcomb-based dual-comb spectroscopy [212]. **b**, Silicon-chip-based mid-infrared dual-comb spectroscopy [213]. **c**, On-chip dual-comb source spectroscopy [83]. **d**, Active microcomb atomic spectrometer, using two EO microcombs [214]. **e**, microcomb-based GHz-midinfrared dual-comb spectroscopy [215]. **f**, Atomic spectroscopy with Kerr microcomb [216]

a nanophotonic silicon-on-insulator platform crafted for mid-infrared DCS [213]. It features two coherently mode-locked frequency combs, which cover wavelengths ranging from 2.6 to 4.1 μm and deliver a spectral resolution of 127 GHz (4.2 cm^{-1}). Figure 10c showcases the enhancement in signal-to-noise ratio for absorption spectroscopy across a span of 170 nm facilitated by an integrated dual-microcomb source [83], this mutually coherent source is powered by a singular pump laser and boasts rapid data acquisition. Furthermore, Fig. 10d depicts the application of microcomb technology in sub-Doppler and hyperfine atomic spectroscopy [214]. This technique benefits from the concurrent control over the microcomb repetition rate and the carrier-envelope offset frequency. The spectroscopy employs a cascaded, two-photon transition at 1529 nm in a micro-machined rubidium cell for atomic transitions. Figure 10e demonstrates a GHz-resolution mid-infrared comb that utilizes interleaved difference frequency generation based on a soliton microcomb [215]. Lastly, Fig. 10f presents dual-microspectrometers constructed on a low-loss thin-film lithium-niobate-on-insulator platform which ensures frequency agility and promotes spectrally-tailored multiplexed spectroscopy [216]. This setup allows for the injection of multiple continuous wave lasers into the system, thereby enabling a broad and flexibly controlled spectral coverage.

4.2 Microcomb based LiDAR and imaging

Laser Detection and Ranging (LiDAR), often regarded as the optical counterpart to RADAR, is an essential technology propelled by the burgeoning field of autonomous vehicles. These systems necessitate real-time updates of three-dimensional (3D) distance measurements and velocity tracking. With advancements in chip-scale nanophotonics, microcombs have emerged as a powerful tool for achieving rapid, precise, and long-range measurements, marking significant progress in the domain of optical comb ranging technology. Typically, LiDAR systems that leverage microcombs can be classified into several types using different analysis schemes: time-of-flight (ToF), frequency-modulated continuous-wave (FMCW), dispersive interferometry (DPI), and random-modulated continuous wave (RMCW).

ToF LiDAR operates by gauging the duration taken by a wave to traverse the distance from the source to the target and back. This approach is prevalent in ranging applications. In 2018, Trocha et al. showcased an accurate and ultrafast ranging system that utilized the ToF technique coupled with two soliton microcombs. This setup achieved in-flight sampling and swift ranging of projectiles traveling around 150 m/s, delivering a lateral resolution of approximately 2 μm and an acquisition rate near 100 MHz [217], as Fig. 11a shows. Moreover, the implementation of two counterpropagating soliton microcombs produced from a single silica wedge

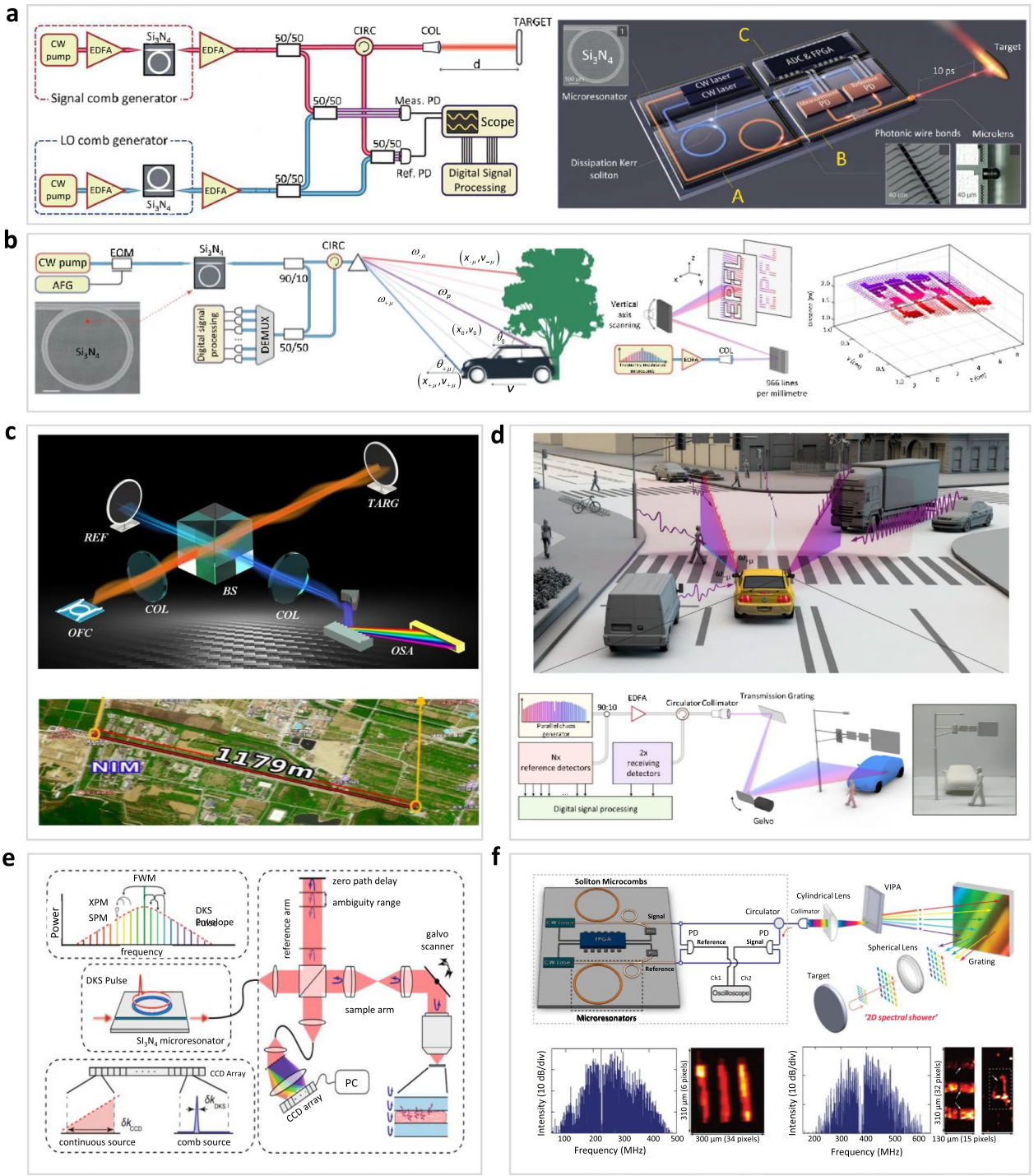

Fig. 11 Microcomb-based LiDARs. **a**, ToF LiDAR based on dual soliton microcomb [217]. **b**, FMCW LiDAR based on single soliton microcomb [220]. **c,** DPI LiDAR based on a Kerr microcomb [222]. **d**, RMCW LiDAR using a chaotic microcomb [224]. **e**, Dissipative Kerr soliton enabled spectral domain optical coherence tomography (OCT) [228]. **f**, Dual-microcomb imaging using microresonator solitons [229]

resonator allowed for the realization of a ToF LiDAR system with a remarkable precision of roughly 200 nm over a half-second averaging period [218]. Furthermore, Jang et al. advanced the precision of such systems by employing spectrally resolved interferometry between reference and measurement pulses, alongside a single soliton

microcomb [219]. This technique mapped information onto the optical ToF and achieved an impressive precision of 3 nm across a 23 mm unambiguous range, maintaining precise metrology for durations exceeding 1000 s.

FMCW LiDAR, which converts distance information into frequency variations using frequency-chirped waveforms, captures the velocity of objects through Doppler frequency shifts identified in the reflected laser beam following a delayed homodyne detection process. This technology achieves high resolution that depends on the extent of the chirp excursion, and does so without the necessity for high-bandwidth electronics. In 2020, Riemensberger and colleagues showcased an advanced parallel coherent FMCW LiDAR system [220]. This was achieved by rapidly varying the frequency of the pump laser and transmitting the chirped signal to each spectral comb tooth within a soliton microcomb. Such an approach allows for the simultaneous measurement of both the distance and velocity of three-dimensional objects, vastly improving frame rates by orders of magnitude as illustrated in Fig. 11b. Building on this concept, Lukashchuk et al. introduced a hardware-efficient methodology utilizing a dual-soliton microcomb that performs coherent ranging and velocimetry at megapixel per second line scan speeds, reaching measurement rates of 5.6 megapixels per second across more than 64 optical channels [221].

DPI LiDAR, tailored for long-range measurements, deciphers distance by analyzing interference spectrum envelopes. Its robustness against interference and extended coherent lengths make it particularly effective for greater distances. However, conventional DPI LiDAR systems encounter a measurement dead zone caused by the disparity between the spectrum analyzer's resolution and the repetition rate of the frequency comb. To overcome this limitation, high-repetition-rate optical microcombs have been employed, effectively eliminating the dead zone and thus enabling DPI-based LiDAR to perform long-distance ranging accurately. In 2021, Wang and collaborators have demonstrated a DPI LiDAR powered by an on-chip soliton microcomb [222], achieving a remarkable long-range detection capability of up to 1179 m during real-time high-speed measurements, with an impressive minimum Allen deviation of 5.6 μm and an operation time averaging 0.2 ms, as showcased in Fig. 11c. Additionally, they proposed a multi-pulse train interference technique that effectively resolved the issue of overlapping cross-correlation interference fringes, enhancing the measurement accuracy to 384 nm over a 1.5 m range [223].

RMCW LiDAR, which pinpoint the apex of the correlation trace from a randomly modulated signal, are well-suited for scenarios characterized by substantial optical disturbances or when multiple devices are operating concurrently within a confined area. In 2023, the development of an incoherent, highly parallel LiDAR was accomplished through the employment of a chaotic microcomb [224]. This technological advancement made use of the innate random modulation of both amplitude and phase present in the chaotic comb lines, thus achieving a ranging precision at the millimeter scale and a velocity resolution at the level of millimeters per second, as depicted in Fig. 11d. In a similar vein, Lukashchuk and colleagues successfully showcased a modulator-free, massively parallel RMCW LiDAR system powered by a chaotic microcomb [225]. This system is capable of delivering clear-cut distance and velocity data with an impressive resolution of approximately 10 cm, a feat made possible due to its distinct noise bandwidth of around 1 GHz.

Based on this as a partial foundation, microcombs have been recently deployed in innovative ways within imaging applications. Frequency comb sources are well-established in optical telecommunications, but for biomedical and Raman imaging techniques like optical coherence tomography (OCT), near-infrared spectral microcombs are essential. Addressing this, Karpov et al. engineered a Si_3N_4 microring resonator's dispersion properties to create an octave-spanning soliton microcomb that extends down to 776 nm, which falls within the optical biological imaging window, by utilizing a 1 μm laser light drive [226]. Their efforts demonstrated potent imaging capabilities. Building on this development, Ji et al. unveiled a microcomb-based light source for OCT that boasts a conversion efficiency of 30% in a non-phase locked regime. This system is compatible with standard commercial spectral domain (SD) OCT systems and capable of imaging human tissue with quality comparable to that achieved by conventional benchtop sources, offering a route toward fully integrated OCT systems [227]. The low-noise characteristics of soliton microcombs further enhance the imaging speed and performance in microcomb-based OCT systems [228], surpassing results obtained from systems employing superluminescent diodes or incoherent microcomb states (Fig. 11e).

Imaging beyond OCT also benefits from microcomb applications. Bao et al. employed a novel image retrieval technique using two frequency combs, circumventing the need for array sensors based on charge-coupled device (CCD) and complementary metal oxide semiconductor (CMOS) technologies [229]. This method achieved imaging of static targets, like the USAF 1951 resolution test chart, and monitored the flow of microparticles within a fluid cell, as Fig. 11f shows. In another creative

application, a research team merged dual optical comb technology with digital holography. This synergy harnessed the broad spectrum and high mutual temporal coherence inherent in dual optical comb technology to facilitate high-precision three-dimensional digital holographic reconstructions [230].

4.3 Microcomb based photonic sensing

Microcomb devices, being compact and highly coherent oscillators, can be employed to develop and operate photonic sensors with exceptional sensitivity and the capability to handle multiple channels. Typically, an unmodified microcomb device is not responsive to external environmental changes. However, by functionalizing the microresonator [231], the frequency combs produced within can exhibit remarkable sensitivities to various physical or chemical parameters. Or, by using a microcomb as the light source, one can create a novel sensing system. This functionalization on microresonator can be achieved through modifications in materials or structure. For instance, to sense force, the comb-tuning microresonator should be designed with mechanical flexibility. For biochemical target detection, one could utilize the evanescent waves in a WGM microcavity and coat the microresonator's surface with a material that enhances its sensitivity. In practical applications, microcomb-based sensors can be classified into two categories: single-point sensors, which are compact in size; and distributed sensors, capable of monitoring parameters across a wider area.

Incorporating a sensitive material within a microcavity, the frequency comb generated inside can be directly utilized as a biochemical sensor [232]. Since 2019, the synergy between frequency combs and microcavities has been explored for sensor applications [233]. Utilizing interference phase measurements, Knoerzer and colleagues developed a refractive index sensor with a detection limit as low as 3.70×10^{-7} RIU (see Fig. 12a). Furthermore, microcombs have been employed to augment the capabilities of integrated photonic biosensor platforms [234]. A notable advancement involves functionalizing an over-modal microresonator with a graphene monolayer, facilitating the creation of a microcomb sensor distinguished by its high chemical selectivity and sensitivity [95, 235]. The adsorption of gas molecules on graphene alters the Fermi level, leading to spectral changes in the high-order soliton frequencies and their beat notes. This provides a powerful method for detecting gas mixtures and monitoring trace single-molecule dynamics. Such an optical microcomb sensor is now available in a compact form, packaged in a plug-and-play box roughly 10 cm in size that incorporates a pump laser diode, polarization controller, microcavity, and photodetector, as depicted in Fig. 12b. In a separate study, An and colleagues explored how a comb pulse train can evoke electrically tunable four-wave mixing in a graphene-based D-shaped fiber heterostructure [236]. The idler signal produced by the comb retains the source's repetition frequency, resulting in a beacon with minimal intensity noise. With additional electrical filtering and lock-in amplification, this sensing system demonstrates capability in detecting ammonia and carbon dioxide gases down to the level of individual molecules. Beyond biochemical detection, microcombs have also been applied to mechanical signal recognition. As illustrated in Fig. 12c, in 2021, Zhang et al. showed that optomechanical dissipative soliton combs produced in a microresonator can identify low-frequency vibrations from a cantilever tip induced by external electric pumping circuits [237]. In 2023, Qin et al. introduced a technique where orthogonal soliton microcombs in a mechanically pliable fiber cavity are used to detect forces and pressures with high sensitivity (down to the sub-nanonewton scale) and a broad dynamic range (up to 7.33 mN) [122]. This achievement is realized through the measurement of carrier frequency offsets between two distinct microcombs.

Microcombs are proving to be valuable not only as one-point sensors but also in the realm of distributed sensing methods. A prime example is the innovative Φ-OTDR technique introduced by Soriano-Amat et al., which utilizes dual-comb spectrometry for fibre interrogation and precise sampling of backscattered light [238]. By incorporating a frequency comb into fiber distributed acoustic sensing, the approach enhances measurement resolution, mitigates existing trade-offs, and suggests that strategic adjustments in the signal generation stage of the comb could significantly lower costs for systems where high levels of acoustic sampling are not crucial (see Fig. 12d). An electrical modulation-based microcomb has also been deployed in a Brillouin optical time domain analyzer (B-OTDA), with impressive outcomes [239]. Utilizing a frequency comb as the probe wave has proven to suppress pulse distortion and lessen non-local effects, which are key factors in broadening the sensing range. In a cutting-edge development of 2024, Li et al. detailed a state-of-the-art application: a dual-comb-based coherently-parallel distributed acoustic fiber sensor (DAS) [240]. This pioneering design permits the linear amalgamation of sensor signals in proportion to the number of comb lines, culminating in an extraordinary leap in sensitivity, straightforward fading attenuation and a capacity for high-powered, Brillouin-free transmission that markedly expands the sensing distance, refer to Fig. 12e. By employing 10-line comb pairs, the

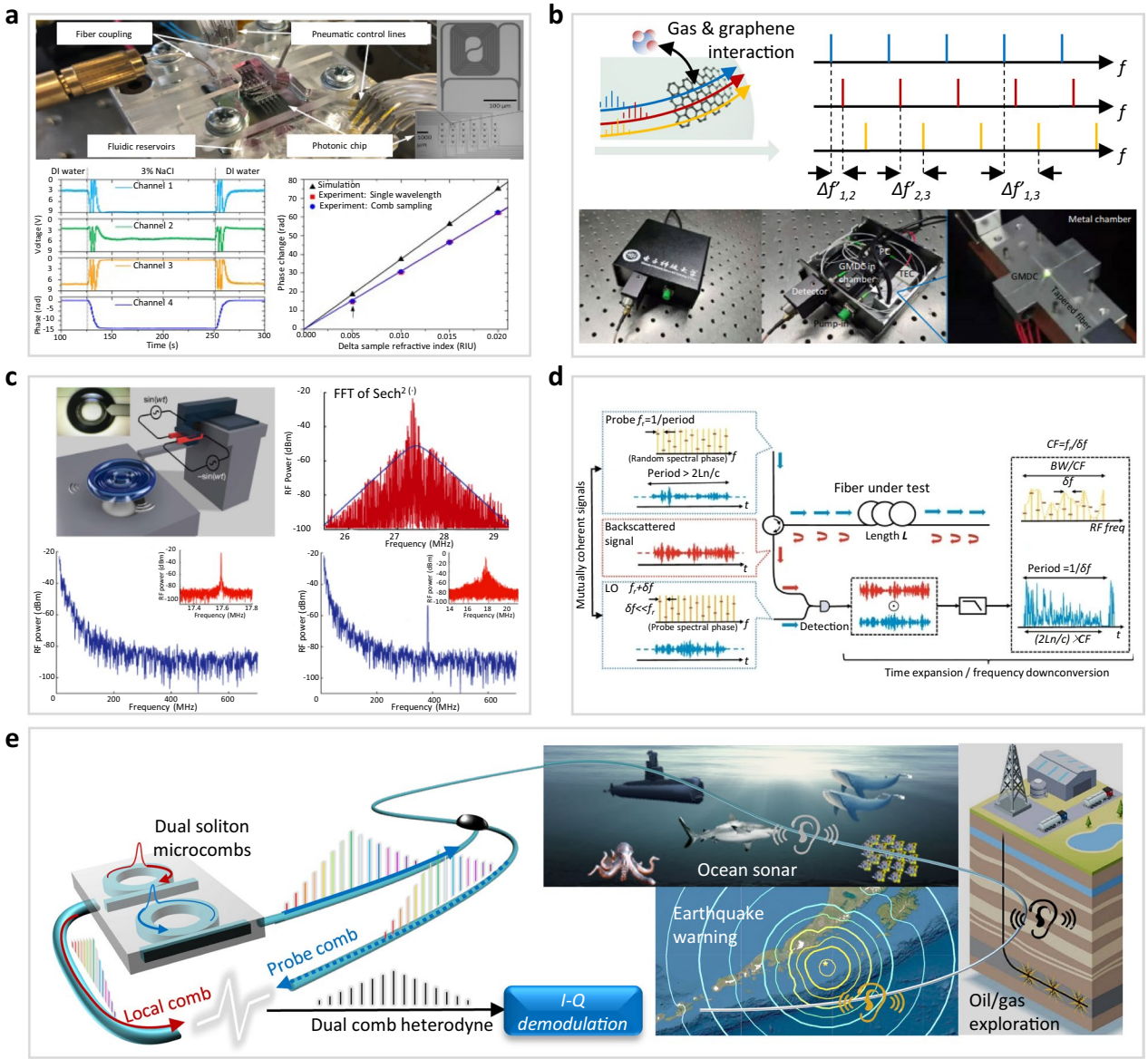

Fig. 12 Microcomb based sensing applications. **a**, Optical frequency comb based photonic refractive index sensor [233]. **b,** Multispecies and individual gas molecule detection using microcomb solitons in a graphene over-modal microresonator [95]. **c**, Detection of a low-frequency vibration of a cantilever tip using optomechanical soliton microcomb in a microtoroid [237]. **d,** Dual EO microcomb source enhances spatial resolution in a fiber distributed sensing system [238]. **e**, On-chip dual Kerr microcomb based ultrasensitive distributed acoustic sensor [240]

researchers established a world-leading detection threshold of 560 femtostrain (fε) per square root hertz at 1 kHz, combined with a 5-m spatial resolution. Here fε means that the strain changes the fiber length by 10^{-15}. This fusion of dual-microcomb metrology with DAS technology heralds a new era of ultra-sensitive DAS capable of achieving femtostrain-level sensitivity per square root hertz, paving the way for the advent of advanced distributed geophones and sonars.

5 Microcomb based information processing

Microcombs are highly promising for information processing due to their ability to produce a vast number of coherent, equidistant frequencies that act like a coherently parallel light source. Therefore, in time domain, microcombs output ultrafast and ultranarrow pulses which contains considerably high peak power. This offers a tool to achieve energy conversion from photon to photon, or from photon to electron, with low threshold, low

consumption, low noise but high efficiency, and thus enables complex information processing linearly or non-linearly. In RF processing, the down conversion combs can be used for filtering or transforming RF signals; in optical logic operation, microcombs can work as pumps and probes in a wide band and generate nonlinear signals; for photonic computation and particularly in convolutional neural networks (CNNs), microcombs can facilitate parallel processing of multiple wavelengths, leading to ultra-fast, high-throughput optical computing capabilities within a compact size. The dense and stable lines of microcombs allow for simultaneous processing of information channels, making them ideally suited for meeting the demands of high-performance, energy-efficient signal processing and computation in next-generation photonic systems. In this section, we emphasize the microcomb based applications for radio frequency processing, optical signal conversion and photonic computation.

5.1 Microcomb based radio frequency processing

The advancement of photonic integrated circuits (PICs) has propelled microwave photonic (MPW) technologies to new heights [241], enabling enhanced light-matter interactions within minuscule footprints across various material platforms [242]. Noteworthy breakthroughs feature external cavity lasers with narrow linewidths, integrated electro-optic modulators with ultrahigh bandwidth capabilities such as thin-film lithium niobate modulators and hybrid organic–plasmonic modulators [243, 244], alongside frequency combs integrated within the circuitry [65], waveguide optical amplifiers [245], and photodetectors [246] boasting exceptional bandwidth, all of which have thrived due to the advancements in semiconductor technology. The exploration of nonlinear optical processes in confined modal volumes has unveiled a plethora of nonlinear effects, including on-chip stimulated Brillouin scattering and frequency doubling [247]. Furthermore, high-density integration techniques, whether monolithic or utilizing multiple materials through hybrid or heterogeneous integration, have become the norm, paving the way for the creation of multifunctional and reconfigurable single microwave photonics processor chips, analogous to their electronic counterparts [248, 249].

Exploration of MWP processors has been carried out utilizing electro-optic and thermo-optic tuning methods as means to achieve controllable optical filtering, differentiation, integration, and Hilbert transformation [250]. These processes are implemented using materials such as indium phosphide, silicon nitride, silicon-on-insulator, gallium arsenide (GaAs), and lithium niobate. The devices are structured in various topologies, including triangular, hexagonal, and square meshes [251–253]. Core components that form the foundation of these systems include phase modulators, tunable couplers, ring resonators, Mach–Zehnder interferometers, and thermal-optic heaters. The progression in this field has positioned integrated MWP technology as a leading solution, addressing challenges such as size, reliability, and cost-effectiveness. Recent innovative demonstrations majorly include the use of a soliton microcomb functioning as a high-quality multiwavelength optical source. This has furthered capabilities in microwave generation [254] and enabled advanced applications like tapped-delay-line microwave photonic filtering [255], true-time delay beamforming [256], arbitrary waveform generation [257], RF channelization [258], and analog signal processing [259]. These advancements underscore the dynamic nature of MWP processors in modern photonic systems.

The demonstration of reconfigurable photonic filters, which leverage the inherent flexibility of soliton dynamics such as pristine soliton crystals and complex soliton formations, is achieved without the need for programmable pulse shaping. By manipulating the relative azimuthal angles during the round-trip cycles, as well as tuning the number of cycles themselves, both the passband frequencies and the shape of the filter can be dynamically adjusted [260], as depicted in Fig. 13a. Furthermore, scientists illustrated a single-bandpass photonic RF filter utilizing a discrete-wavelength comb source, which offers a tunable center frequency alongside a shape that can be programmed [255]. Progressing to beamforming, we demonstrate a true-time delay approach in Fig. 13b. In this work, binary-coded notch filters and RF equalizing filters are successfully realized, which come with adjustable slopes, bandwidths, and center frequencies [261]. Refinement continues in the form of an adaptable intensity differentiator, which boasts variable differentiation orders and is presented in Fig. 13c. This device's capabilities are a result of precise programming and shaping of individual comb lines informed by calculated tap weights [262]. In the domain of RF photonics, a fractional Hilbert transformer with flexible features is showcased in Fig. 13d. This transformer allows for adjustable bandwidths, selectable fractional orders, and switchable center frequencies, all the while offering broad operational bandwidth [263, 264]. Lastly, we demonstrate a broad-spectrum RF channelizer that integrates microring filtering with a broad soliton microcomb in Fig. 13e. The reliability of microwave photonic processing is somewhat constrained by tap errors as well as power fluctuations in the comb lines that occur during comb shaping [265, 266]. To counteract these limitations, a real-time feedback control path is employed, enhancing the system's performance through error minimization.

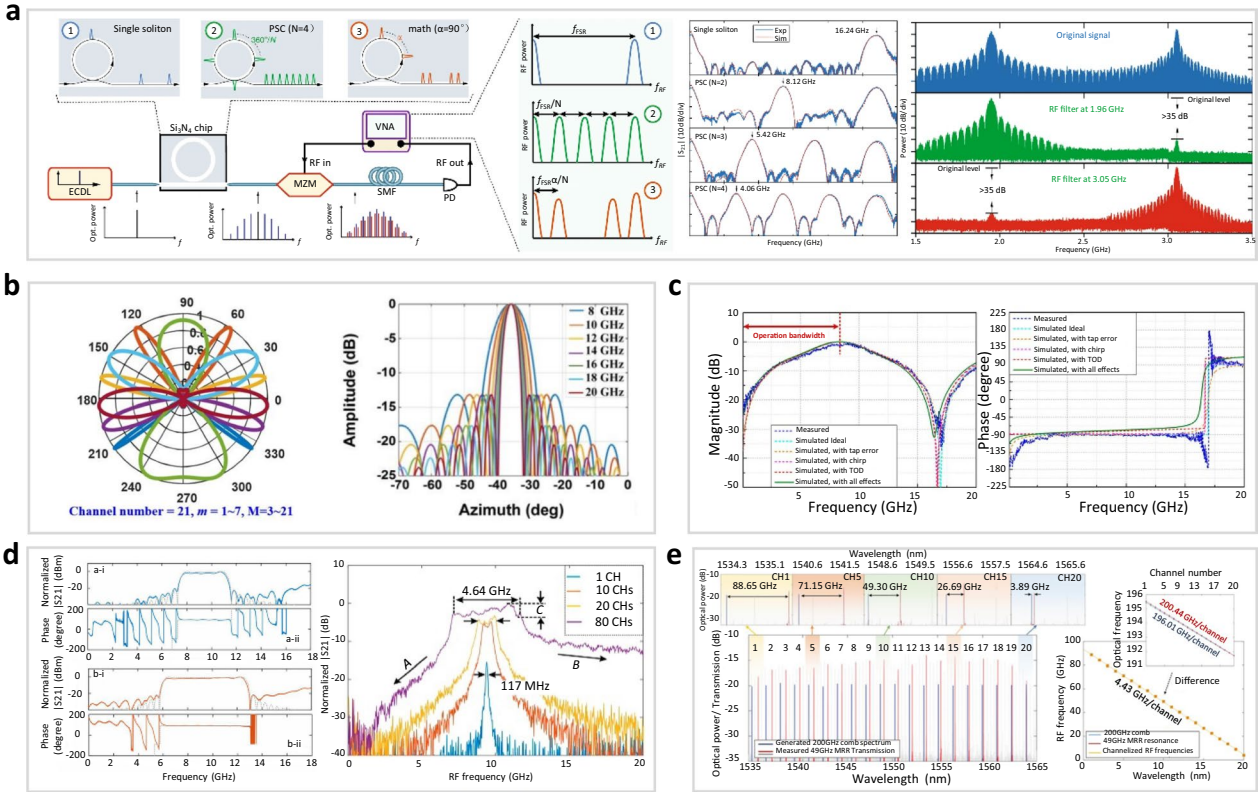

Fig. 13 Microcomb contributes in frequency processing. **a**, Reconfigurable narrow bandwidth filter [260]. **b**, Tunable delay line for beam steering [261]. **c**, Intensity differentiators [262]. **d**, Hilbert transformer and bandwidth tunable RF [263, 264]. **e**, Microcomb based broadband RF channelizer [266]

5.2 Microcomb based nonlinear conversion

Microcombs also show great promise as a versatile optical source for use in optical nonlinear conversion (such as new frequency excitation). One of their superiorities lies in their ability to generate a broad spectrum of frequencies from a single laser source with remarkably narrow linewidth, allowing efficient and accurate frequency conversion and mixing without increasing complexity or footprint. Therefore, microcombs help to address the need for the compact, stable, low-noise, high-coherence and high-resolution sources for advanced nonlinear processing techniques. The most important characteristics of microcombs in these contexts include their phase coherence, low phase noise, and the ability to tailor the comb's spectral bandwidth and line spacing. These attributes directly translate to improved performance and offers better accuracy and resolution while minimizing the size and power consumption of the equipment.

Being highly-coherent pulsed lasers, microcombs naturally stand as ideal light sources for nonlinear conversion, particularly in scenarios requiring both high peak power and precise time–frequency calibration, such as pump-probe experiments [267]. These devices offer multiple channels that facilitate filtering, which presents distinctive advantages in the exploration of parametric nonlinear optics with layered materials and their corresponding heterostructures, as well as in the controlled generation of terahertz radiation [268, 269]. Serving as a nonlinear control laser, recent research has indicated that a frequency comb can deliver ultrafast energy to enhance terahertz transparency in meta-cavities [270]. When utilized as the pumping source for second-harmonic generation (SHG), third-harmonic generation (THG), and sum-frequency conversion, there have been demonstrations of cascaded frequency comb conversions within the visible spectrum [43]. Specifically, Jung et al. showcased the excitement of comb-like visible frequency lines by a Kerr comb operating in a high-Q aluminum nitride microring resonator, leading to sequential frequency conversions in visible band (Fig. 14a). Moreover, this work illuminated visible frequency comb generation accompanied by pronounced Cherenkov-like radiation, achieving an on-chip nonlinear conversion efficiency of 22% [271].

Building upon the dissipative Kerr soliton and cascaded Brillouin stimulation, Zhang et al. reported the simultaneous generation and multiplexing of several comb

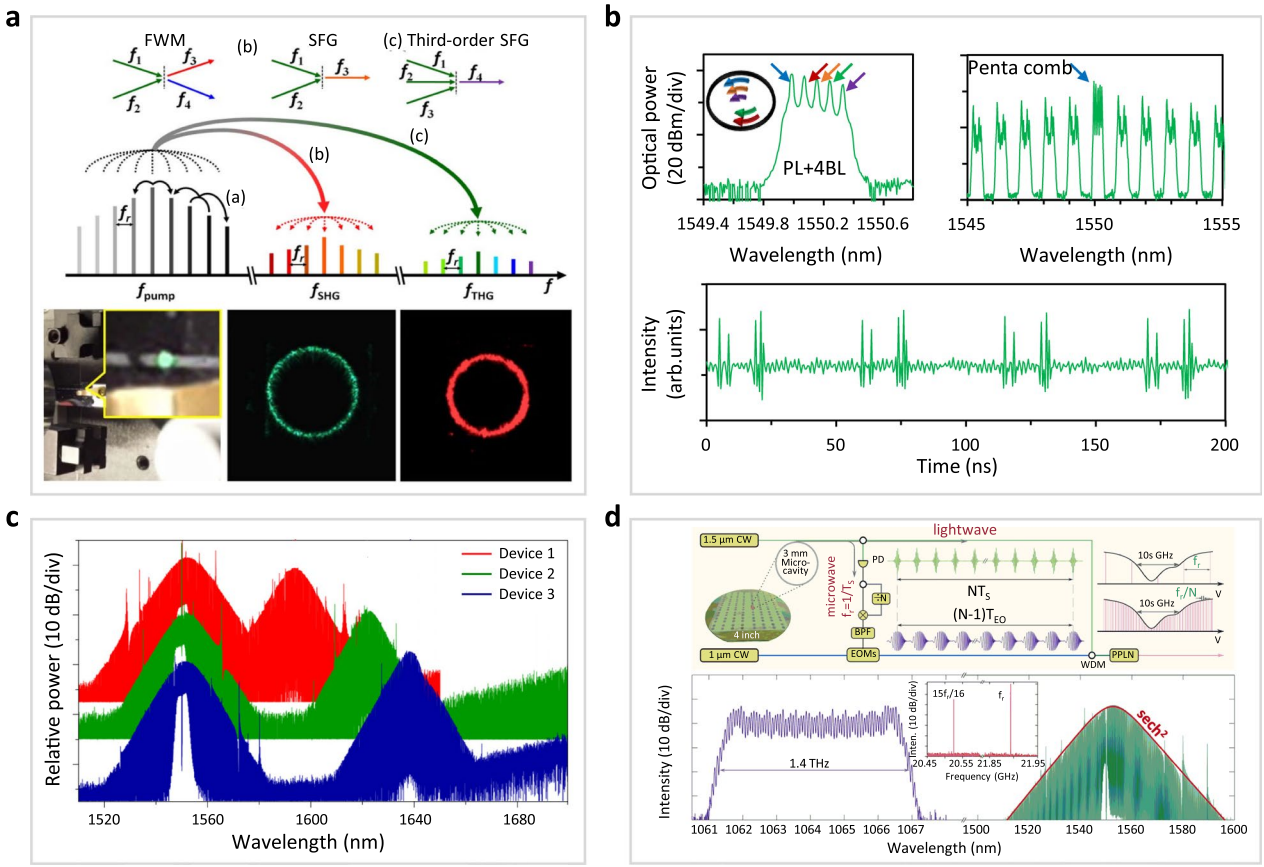

Fig. 14 Microcomb based nonlinear conversion and imaging. **a**, NIR to visible frequency conversion using a microcomb [43]. **b**, Multiplexing of soliton microcombs using cascaded Brillouin excitation [272]. **c**, The measured primary and Stokes soliton spectra corresponding to three different devices [105]. **d**, Interleaved difference-frequency generation (iDFG) experimental setup and the optical spectra of the near-IR EO-comb (left) and soliton microcomb (right) [273]

families within a single over-modal microresonator [272]. By strategically choosing the primary comb frequency, they achieved the emergence of up to five solitons in both clockwise and counter-clockwise directions, which provided radio frequency carrier signals across a spectrum exceeding 40 GHz, as depicted in Fig. 14b. Expanding beyond Brillouin effects, a microcomb produced at the communication band (1550 nm) has the capacity to generate a coinciding Stokes microcomb within the U-band (1650 nm) (Fig. 14c) [105]. Furthermore, when paired with difference frequency generation for the intensification of near-infrared to mid-infrared (NIR-MIR) frequencies, a microcomb serves as a proficient light source (Fig. 14d) [273]; and for plasmon generation, two microcombs with significant wavelength separation could potentially function as counter-propagating pumps [274].

5.3 Microcomb based optical computation

Optical computing systems are known for delivering high-speed, power-efficient hardware solutions for information processing, outperforming their electronic counterparts. These systems have emerged as a compelling approach to address the fundamental bandwidth limitations inherent in traditional electronic systems. Over the last decade, significant interest has been garnered in all-optical and optoelectronic signal processing techniques [275]. Despite this interest, there was a prolonged anticipation for the development of multi-channel light sources with high repetition rates and superior coherence. Presently, microcombs have risen to prominence as an effective tool, offering multiple parallel signal channels that enhance information processing capabilities. This is evident in their applications, particularly in advanced neuromorphic computing and programmable logic operations [80, 276].

In 2021, large-scale parallel computing utilizing microcombs was introduced in the context of optical neural networks (ONNs) [277]. The pivotal work of Feldmann et al. showcased a photonic tensor core specifically designed for computation. This core operates at the

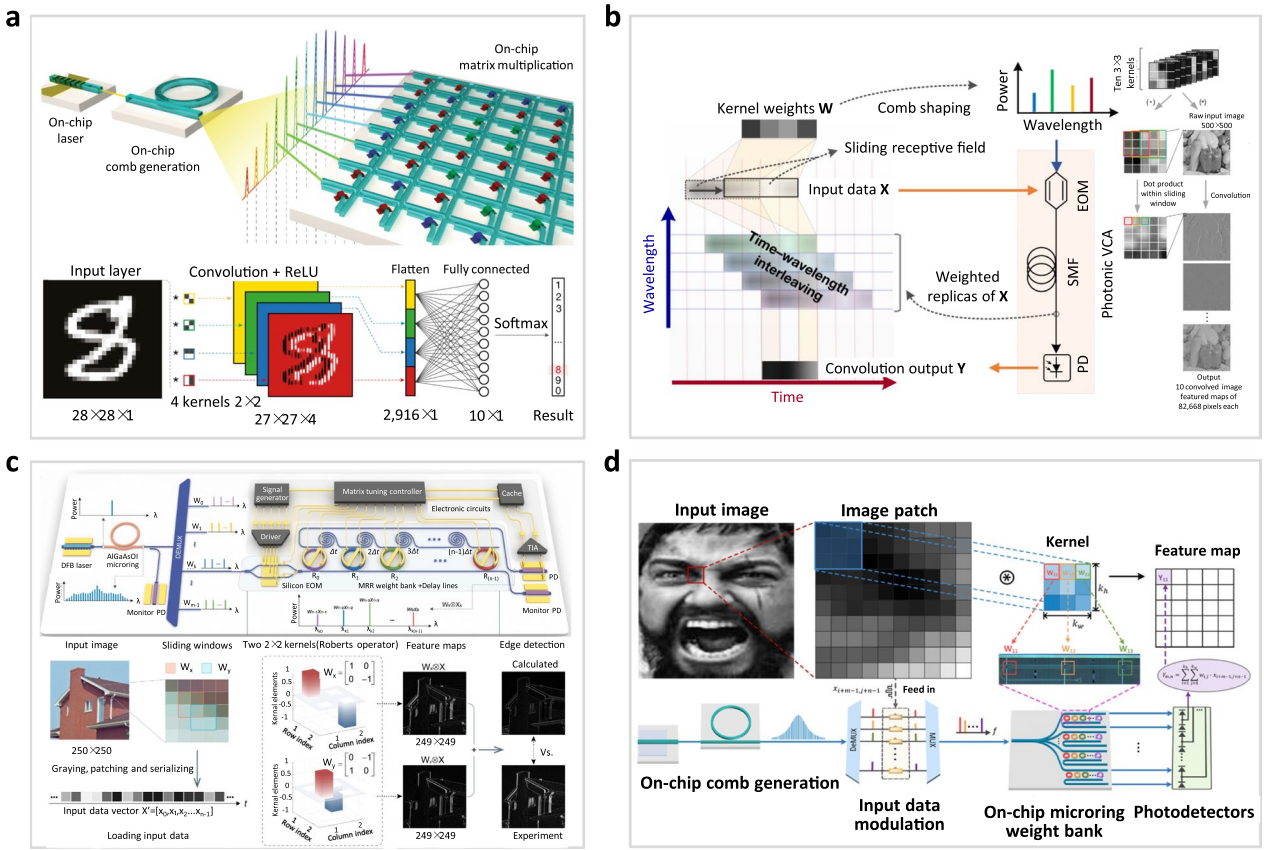

Fig. 15 Microcomb based optical computation. **a**, Microcomb-based convolution computation accelerator [277]. **b**, Operation principle of an optical CNN based on time–wavelength interleaving using a soliton crystal microcomb [278]. **c**, Microcomb-based integrated photonic processing unit [279]. **d**, Microcomb-enabled integrated optical neural network [280]

speed of trillions of multiply-accumulate operations per second. Utilizing phase-change material memory arrays and soliton microcombs on a photonic chip, it conducts photonic in-memory computing in a parallelized manner. The core features an operational bandwidth that surpasses 14 gigahertz and exhibits potential for integration with CMOS-based wafer-scale technology (see Fig. 15a). In a simultaneous study, Xu et al. demonstrated the capability of a microcomb to transfer information for a universal optical vector convolutional accelerator [278]. This system operates at speeds exceeding 10 TOPS and can process image convolutions for images up to 250,000 pixels in size, which is substantial enough for tasks such as image and video recognition (Fig. 15b). Progressing to 2023, Bai et al. reported further advancements in optical convolution by employing a time-wavelength plane stretching method within a microcomb-driven chip-based photonic processing unit [279]. This development achieved unprecedented precision of 9 bits and processing speeds over 1 TOPS per square millimeter, as depicted in Fig. 15c. Expanding upon these findings, Chen et al. implemented a microcomb-enabled integrated optical neural network (MIONN) architecture [280]. This system is capable of processing large-sized images with a throughput of 51.2 TOPS and energy efficiency measured at 4.18 TOPS/W. Furthermore, it has successfully been used for human emotion recognition with a commendable accuracy of 78.5% (Fig. 15d).

These advanced computing methodologies utilizing microcombs offer significant promise, transcending the capabilities of electronic devices and heralding a new era of photonic AI. Beyond the previously noted applications in Optical Neural Networks (ONNs), the ultra-stable, low-jitter characteristics of microcombs are set to transform existing digital technologies, significantly enhancing the effective resolution of bits [281]. Moreover, microcombs can be employed for facilitating information exchange in the context of electro-optical logic gates [274], paving the way for diverse optical computing architectures, both analog and digital [282]. This is achievable by customizing the comb lines in optical signal processing (OSP), creating adaptable linear and nonlinear filters suitable for tasks such as correlation, equalization, and

Volterra filtering. Additionally, these systems facilitate the design of dynamic bandwidth allocation schemes.

6 Discussion and outlook

The field of microcombs has reached a pivotal juncture following substantive strides in device development and system-prototype showcases. Firstly, numerous comb-generation techniques have yielded noteworthy performance benchmarks for devices, with several reaching parity with larger-scale instruments, prompting the exploration of initial system-level applications. Secondly, considerable challenges persist that require resolution to fulfill the potential advantages of microcombs and to facilitate this technology's migration into industrial and commercial manufacturing domains. Lastly, there are trade-offs among multi-dimensional parameters within various informational applications, including power versus efficiency, speed versus spectral density, as well as stability versus controllability.

One critical problem is the power. Amplification currently stands as a major limiting factor hindering further integration of these systems. The erbium-doped fiber amplifier (EDFA) is a prevalent solution, employed at both the input and output stages of the system. However, the use of EDFA increases energy consumption, introduces amplified spontaneous emission noise, and is confined to a limited amplification bandwidth [283]. On the other hand, integrated semiconductor optical amplifiers present an alternative, capable of boosting comb power to levels on par with discrete on-chip lasers (in the milliwatt range). Nonetheless, they are similarly restricted by a narrow spectral bandwidth, typically under several tens of nanometers [284]. Furthermore, both amplification methods mentioned above do not enhance the optical signal-to-noise ratio. This is particularly considered for broadband microcomb generation, such as *f-2f* or *2f-3f* applications, where the required pump power and nonlinear conversion efficiency are still insufficiently high. In response to this issue, new developments have emerged in recent years. For instance, the Vernier dual-comb configuration [285], injection-locking, and Kerr-induced synchronization [144, 286] have been utilized for the self-referencing of Kerr combs. This technique allows an external laser to capture a comb tooth with a sub-milliwatt laser. When combined with an octave-spanning comb, the synchronization enables amplifierless f_{ceo} detection by using a state-of-the-art integrated second-harmonic generation element [287]. Looking forward, innovative solutions may lie in the combination of active assistance with passive microresonators [288], in-cavity or on-chip chirped pulse amplification [289], and the implementation of miniaturized on-chip mode-locking techniques [290]. These approaches could potentially overcome the current limitations in microcomb system amplification.

The complexity of microcomb setups presents another significant challenge, demanding higher standards for reliability, manufacturing, and cost-efficiency in comparison to conventional fiber mode-locked lasers. For instance, generating a stable Kerr soliton microcomb on-chip typically requires the use of a narrow linewidth external cavity laser as the pump, along with an auxiliary laser for thermal shift management, and a precise process to transition the pumping frequency from blue-detuned to red-detuned regions in a resonance [30]. The intricate phenomena involved in comb formation often result in various comb states, which can cause notable instability during operation [84]. Commonly, there is a need for comprehensive monitoring and control capabilities to manage comb operation effectively. Fortunately, by utilizing turnkey operations through self-injection mode-locking [86], slingshot effects based on photonic crystals and mode crossing [64, 288], as well as their combination [291], one can effectively bypass the need for meticulous monitoring. In the future, heterogeneous integration of multiple devices [17, 292] or employing less integrated yet still packable versions [70] will also be powerful approaches.

Moreover, different applications necessitate specific comb characteristics. For instance, in optical communication, a small repetition frequency is desired to fulfill high-density wave-multiplexing requirements and low phase noise is critical for minimizing bit error rates [168]. Conversely, applications like terahertz generation and spectroscopy demand microcombs with a broad span, large frequency intervals, and high power in each comb line [18]. Other uses such as sensing, LiDAR, and computation require seamless switching and precise inter-mode controllability [59, 95]. As scenarios where multiple applications converge are poised to become more prevalent in the future, one key technical challenge lies in integrating microcombs with varying characteristic parameters to meet diverse needs effectively, which will be a complex yet valuable undertaking to pursue.

Figure 16 illustrates the key parameters of various microcomb types, while Table 1 catalogs the comb types employed in different information technology applications. These combs originate from assorted platforms and exploit diverse physical mechanisms. The information in the table is taken from Sects. 3, 4, 5. While an all-encompassing solution for comb generation that excels across all parameters would be ideal [7], practical advancements in microcomb technology are primarily driven by specific applications. Consequently, the integration of benefits

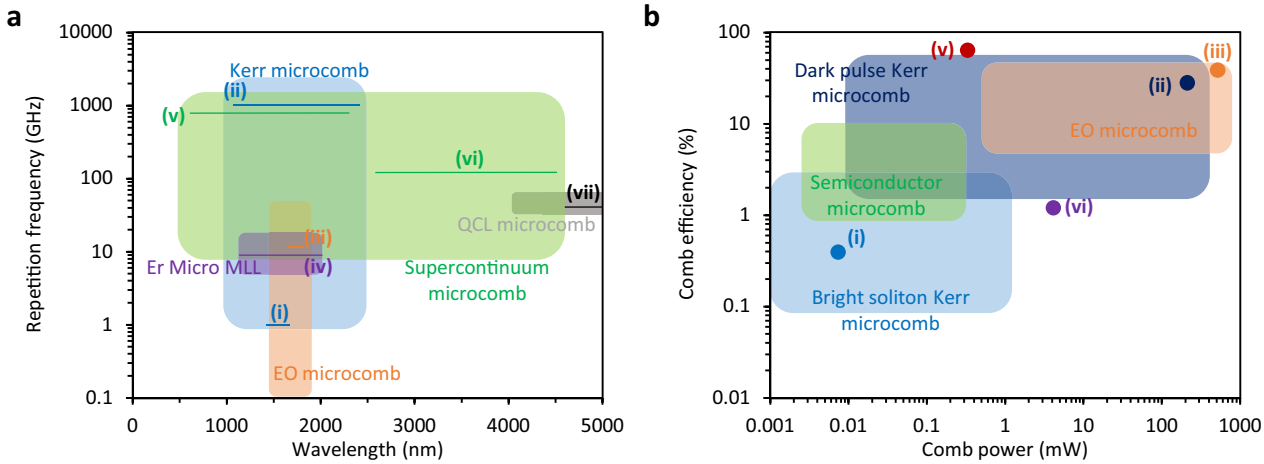

Fig. 16 Different microcomb schemes with distinct parameters. **a**, Microcombs with varied optical spans and repetition rates. Examples are showed in colored lines: (i) a Kerr soliton microcomb generated in a fiber F-P cavity [122], (ii) an octave-spanning microcomb in a Si_3N_4 microresonator [293], (iii) A resonant EO comb generated in LN ring [77], (iv) a mode locked laser comb pulsed by graphene heterostructure [60], (v) a chaos assisted microcomb [63], (vi) a silicon-chip-based mid-infrared microcomb [213], (vii) a mid-infrared frequency comb from a ring quantum cascade laser [294]. **b,** Microcombs with varied comb power and efficiency. Examples are showed in colored dots: (i) A typical bright soliton microcomb generated in a high *Q* silica microcavity with FSR = 22 GHz [26], (ii) a dark-pulse generated in a normal dispersion microresonator with FSR = 100 GHz [109], (iii) a high efficiency EO microcomb with repetition 25 GHz [295], (iv) an ultra-efficient microcomb in an AlGaAs microresonator with FSR = 1 THz [45], (v) a soliton microcomb with surpassing conversion efficiency, FSR = 50 GHz [112], (vi) a photonic integrated high-power soliton microcomb using on-chip erbium amplification [296]

Table 1 Applications using different microcombs

Application		Comb type	Key features	Representative advances	Refs.
Information carrier	Microwave signal generation	Kerr soliton microcomb on chip	Wavelength C + L band Repetition 16 ~ 227 GHz	46 dB phase-noise reduction	[156]
	Frequency synchronization	*f-2f* soliton microcomb on chip	f_{ceo} 10^{-13}/s f_{rep} 10^{-15}/s	External reference free	[33]
	Data transmission	Coherence-cloned DKS microcomb	1550 nm Repetition 100 GHz	55 Tbit/s BER: 3.8e−3	[168]
	Quantum excitation and transition	Kerr soliton microcomb	40 GHz repetition	> 50 entangled photon pairs	[193]
Information acquisition	Spectroscopy	Supercontinuum dual microcomb	Span covers 1 μm to > 4 μm	ppm sensitivity	[215]
	LiDAR	Kerr soliton microcomb	Co-generation of dual soliton in one single cavity	Precision in nm level Speed in ms level	[218]
	Imaging	Kerr soliton dual microcomb	Large repetition difference	Frame 200 kHz fill rate 48 Mpixels/s	[229]
	Biochemical sensing	Raman soliton in WGM microcavity	1670 nm, multi-microcomb mixing	Single molecule detection	[95]
	Distributed fiber sensing	EO microcomb On chip dual comb	2.5 GHz repetition (EO) 100 GHz repetition (soliton)	cm spatial resolution 560 fε/Hz$^{1/2}$ sensitivity	[240]
Information processing	Radio frequency processing	On chip microcomb	Programmable pulse shaping	> 10 signal processing functions	[255]
	Nonlinear conversion	Microcomb in AlN microring	NIR to Visible mode to mode matching	nW level power > 20% efficiency	[43]
	Computation	Soliton microcomb in nitride microring	49 GHz spacing, > 90 comb lines	11 TOPs in CNN	[278]

and the mitigation of weaknesses from different combs represent a significant research direction.

Over the last decade, microcomb technology has surmounted numerous scientific and technical challenges, establishing itself as a reliable resource for a multitude of valuable photonics and optoelectronics applications in a scalable way. Given the swift progress already made, it is expected that the coming decade will witness the deployment of microcombs in extensive photonic integrated circuits and nascent technologies. These advancements promise to benefit sectors such as data transmission, sensing, timekeeping, and information processing in the next generation.

Acknowledgements
The authors thank Yong Geng, Kun-Peng Jia, Yu-Pei Liang, Yun-Ru Fan, and Zhen Tian, for their contributions of formatting, editing and theoretical complements.

Author contributions
B.Y. and W.W. contributed equally to this work. B.Y. led the paper organization. C.W.W. proofed the document. All authors contributed to the writing and approved the final manuscript.

Funding
This research was supported by the National Key Research and Development Program of China (2023YFB2806200, 2021YFB2800602, 2022YFB2802702), the National Natural Science Foundation of China (U2130106, 62305050) and Sichuan Science and Technology Program (2022YFSY0061, 2023YFSY0060), the National Postdoctoral Innovation Talent Support Program of China (BX20220056) and National Science Foundation of the United States (QuIC-TAQS 2137984 and QII-TAQS 1936375).

Availability of data and materials
Not applicable.

Declarations

Competing interests
The authors declare no competing interests.

Received: 5 April 2024 Revised: 30 May 2024 Accepted: 6 June 2024
Published online: 10 October 2024

References

1. S.T. Cundiff, J. Ye, Colloquium femtosecond optical frequency combs. Rev. Mod. Phys. **75**, 325–342 (2003)
2. S.A. Diddams, K. Vahala, T. Udem, Optical frequency combs: Coherently uniting the electromagnetic spectrum. Science **369**, 3676 (2020)
3. A. Tikan et al., Emergent nonlinear phenomena in a driven dissipative photonic dimer. Nat. Phys. **17**, 604–610 (2021)
4. S.B. Papp et al., Microresonator frequency comb optical clock. Optica **1**, 10 (2014)
5. T. Fortier, E. Baumann, 20 years of developments in optical frequency comb technology and applications. Commun. Phys. **2**, 153 (2019)
6. S.A. Diddams, The evolving optical frequency comb. J. Opt. Soc. Am. B **27**, B51 (2010)
7. L. Chang, S. Liu, J.E. Bowers, Integrated optical frequency comb technologies. Nat. Photonics **16**, 95–108 (2022)
8. A. Rueda, F. Sedlmeir, M. Kumari, G. Leuchs, H.G.L. Schwefel, Resonant electro-optic frequency comb. Nature **568**, 378–381 (2019)
9. P. Del'Haye et al., Optical frequency comb generation from a monolithic microresonator. Nature **450**, 1214–1217 (2007)
10. T. Herr et al., Universal formation dynamics and noise of Kerr-frequency combs in microresonators. Nat. Photonics **6**, 480–487 (2012)
11. T. Herr et al., Temporal solitons in optical microresonators. Nat. Photonics **8**, 145–152 (2014)
12. X. Xue et al., Mode-locked dark pulse Kerr combs in normal-dispersion microresonators. Nat. Photonics **9**, 594–600 (2015)
13. T.J. Kippenberg, R. Holzwarth, S.A. Diddams, Microresonator-based optical frequency combs. Science **332**, 555–559 (2011)
14. S.-P. Yu et al., Tuning Kerr-soliton frequency combs to atomic resonances. Phys. Rev. Appl. **11**, 044017 (2019)
15. A. Pasquazi et al., Micro-combs: a novel generation of optical sources. Phys. Rep. **729**, 1–81 (2018)
16. Z. Zhou et al., Prospects and applications of on-chip lasers. ELight **3**, 1 (2023)
17. H. Shu et al., Microcomb-driven silicon photonic systems. Nature **605**, 457–463 (2022)
18. N. Picqué, T.W. Hänsch, Frequency comb spectroscopy. Nat. Photonics **13**, 146–157 (2019)
19. E. Obrzud et al., A microphotonic astrocomb. Nat. Photonics **13**, 31–35 (2019)
20. J. Pfeifle et al., Coherent terabit communications with microresonator Kerr frequency combs. Nat. Photonics **8**, 375–380 (2014)
21. H. Zhang et al., Coherent optical frequency combs: from principles to applications. J. Electron. Sci. Technol. **20**, 100157 (2022)
22. J. Liu et al., Emerging material platforms for integrated microcavity photonics. Sci China Physics Mech. Astron. **65**, 10420 (2022)
23. P. Del'Haye et al., Octave Spanning Tunable Frequency Comb from a Microresonator. Phys. Rev. Lett. **107**, 063901 (2011)
24. T. Hansson, S. Wabnitz, Dynamics of microresonator frequency comb generation: models and stability. Nanophotonics **5**, 231–243 (2016)
25. A. Kovach et al., Emerging material systems for integrated optical Kerr frequency combs. Adv. Opt. Photonics **12**, 135 (2020)
26. X. Yi, Q.-F. Yang, K.Y. Yang, M.-G. Suh, K. Vahala, Soliton frequency comb at microwave rates in a high-Q silica microresonator. Optica **2**, 1078 (2015)
27. L. Yao et al., Soliton microwave oscillators using oversized billion Q optical microresonators. Optica **9**, 561 (2022)
28. D.J. Moss, R. Morandotti, A.L. Gaeta, M. Lipson, New CMOS-compatible platforms based on silicon nitride and Hydex for nonlinear optics. Nat. Photonics **7**, 597–607 (2013)
29. L. Razzari et al., CMOS-compatible integrated optical hyper-parametric oscillator. Nat. Photonics **4**, 41–45 (2010)
30. T. Herr et al., Temporal solitons in optical microresonators. Nat. Photonics **8**, 145–152 (2014)
31. C. Lecaplain, C. Javerzac-Galy, M.L. Gorodetsky, T.J. Kippenberg, Mid-infrared ultra-high-Q resonators based on fluoride crystalline materials. Nat. Commun. **7**, 13383 (2016)
32. S.B. PappHaye, Mechanical control of a microrod-resonator optical frequency Comb. Phys Rev. **3**, 031003 (2013)
33. D.T. Spencer et al., An optical-frequency synthesizer using integrated photonics. Nature **557**, 81–85 (2018)
34. H. Lee et al., Chemically etched ultrahigh-Q wedge-resonator on a silicon chip. Nat. Photonics **6**, 369–373 (2012)
35. T. Tan et al., Predicting Kerr Soliton Combs in microresonators via deep neural networks. J. Light. Technol. **38**, 6591–6599 (2020)
36. M.L. Gorodetsky, A.A. Savchenkov, V.S. Ilchenko, Ultimate Q of optical microsphere resonators. Opt. Lett. **21**, 453 (1996)
37. Y. Guo et al., A monolithic graphene-functionalized microlaser for multispecies gas detection. Adv. Mater. **34**, 2207777 (2022)
38. J.S. Levy et al., CMOS-compatible multiple-wavelength oscillator for on-chip optical interconnects. Nat. Photonics **4**, 37–40 (2010)
39. F. Gyger et al., Observation of stimulated brillouin scattering in silicon nitride integrated waveguides. Phys. Rev. Lett. **124**, 013902 (2020)
40. M. Corato-Zanarella, X. Ji, A. Mohanty, M. Lipson, Absorption and scattering limits of silicon nitride integrated photonics in the visible spectrum. Opt. Express **32**, 5718 (2024)
41. J. Liu et al., High-yield, wafer-scale fabrication of ultralow-loss, dispersion-engineered silicon nitride photonic circuits. Nat. Commun. **12**, 2236 (2021)

42. M.W. Puckett et al., 422 Million intrinsic quality factor planar integrated all-waveguide resonator with sub-MHz linewidth. Nat. Commun. **12**, 934 (2021)
43. H. Jung, R. Stoll, X. Guo, D. Fischer, H.X. Tang, Green, red, and IR frequency comb line generation from single IR pump in AlN microring resonator. Optica **1**, 396 (2014)
44. J. Liu et al., Monolithic piezoelectric control of soliton microcombs. Nature **583**, 385–390 (2020)
45. L. Chang et al., Ultra-efficient frequency comb generation in AlGaAs-on-insulator microresonators. Nat. Commun. **11**, 1–8 (2020)
46. Y. Zheng et al., Integrated gallium nitride nonlinear photonics. Laser Photon. Rev. **16**, 2100071 (2022)
47. D.J. Wilson et al., Integrated gallium phosphide nonlinear photonics. Nat. Photonics **14**, 57–62 (2020)
48. G. Moille et al., Dissipative Kerr Solitons in a III-V Microresonator. Laser Photon. Rev. **14**, 2000022 (2020)
49. L. Wu et al., AlGaAs soliton microcombs at room temperature. Opt. Lett. **48**, 3853 (2023)
50. Y. He et al., Self-starting bi-chromatic LiNbO 3 soliton microcomb. Optica **6**, 1138 (2019)
51. L. Zhang et al., Microdisk resonators with lithium-niobate film on silicon substrate. Opt. Express **27**, 33662 (2019)
52. M. Jankowski et al., Ultrabroadband nonlinear optics in nanophotonic periodically poled lithium niobate waveguides. Optica **7**, 40 (2020)
53. A. Guarino, G. Poberaj, D.D. Rezzonico, R. Innocenti, P. Günter, Electro–optically tunable microring resonators in lithium niobate. Nat. Photonics **1**, 407–410 (2007)
54. M. Zhang, C. Wang, R. Cheng, A. Shams-Ansari, M. Lončar, Monolithic ultra-high-Q lithium niobate microring resonator. Optica **4**, 1536 (2017)
55. C. Wang et al., High-Q microresonators on 4H-silicon-carbide-on-insulator platform for nonlinear photonics. Light Sci. Appl. **10**, 139 (2021)
56. B.J.M. Hausmann, I. Bulu, V. Venkataraman, P. Deotare, M. Lončar, Diamond nonlinear photonics. Nat. Photonics **8**, 369–374 (2014)
57. D. Xia et al., Integrated chalcogenide photonics for microresonator soliton Combs. Laser Photon. Rev. **17**, 2200219 (2023)
58. N. Zhang et al., Highly reproducible organometallic halide perovskite microdevices based on top-down lithography. Adv. Mater. **29**, 1606205 (2017)
59. B. Yao et al., Gate-tunable frequency combs in graphene–nitride microresonators. Nature **558**, 410–414 (2018)
60. C. Qin et al., Electrically controllable laser frequency combs in graphene-fibre microresonators. Light Sci. Appl. **9**, 185 (2020)
61. T. Tan, X. Jiang, C. Wang, B. Yao, H. Zhang, 2D material optoelectronics for information functional device applications: status and challenges. Adv. Sci. **7**, 2000058 (2020)
62. A. Keşkekler, H. Arjmandi-Tash, P.G. Steeneken, F. Alijani, Symmetry-breaking-induced frequency combs in graphene resonators. Nano Lett. **22**, 6048–6054 (2022)
63. H.-J. Chen et al., Chaos-assisted two-octave-spanning microcombs. Nat. Commun. **11**, 2336 (2020)
64. S.-P. Yu et al., Spontaneous pulse formation in edgeless photonic crystal resonators. Nat. Photonics **15**, 461–467 (2021)
65. T.J. Kippenberg, A.L. Gaeta, M. Lipson, M.L. Gorodetsky, Dissipative Kerr solitons in optical microresonators. Science. **361**, eaan8083 (2018)
66. L.A. Lugiato, R. Lefever, Spatial Dissipative Structures in Passive Optical Systems. Phys. Rev. Lett. **58**, 2209–2211 (1987)
67. H. Zhou et al., Soliton bursts and deterministic dissipative Kerr soliton generation in auxiliary-assisted microcavities. Light Sci. Appl. **8**, 50 (2019)
68. S. Zhang et al., Sub-milliwatt-level microresonator solitons with extended access range using an auxiliary laser. Optica **6**, 206 (2019)
69. Z. Lu et al., Deterministic generation and switching of dissipative Kerr soliton in a thermally controlled micro-resonator. AIP Adv. **9**, 025314 (2019)
70. Y. Xiao et al., Optimizing auxiliary laser heating for Kerr soliton microcomb generation. Opt. Lett. **49**, 1129 (2024)
71. L. Zhou, Y. Shen, C. Xi, X. Huang, G. He, Computer-controlled microresonator soliton comb system automating soliton generation and expanding excursion bandwidth. Opt. Contin. **1**, 161 (2022)
72. X. Ni et al., Broadband sheet parametric oscillator for χ (2) optical frequency Comb generation via cavity phase matching. Chinese Phys. Lett. **38**, 064201 (2021)
73. V. Ulvila, C.R. Phillips, L. Halonen, M. Vainio, Frequency comb generation by a continuous-wave-pumped optical parametric oscillator based on cascading quadratic nonlinearities. Opt. Lett. **38**, 4281 (2013)
74. V. Ulvila, C.R. Phillips, L. Halonen, M. Vainio, High-power mid-infrared frequency comb from a continuous-wave-pumped bulk optical parametric oscillator. Opt. Express **22**, 10535 (2014)
75. X. Wang et al., 2 μm optical frequency comb generation via optical parametric oscillation from a lithium niobate optical superlattice box resonator. Photonics Res. **10**, 509 (2022)
76. J.R. Stone et al., Thermal and nonlinear dissipative-soliton dynamics in Kerr-Microresonator frequency combs. Phys. Rev. Lett. **121**, 063902 (2018)
77. M. Zhang et al., Broadband electro-optic frequency comb generation in a lithium niobate microring resonator. Nature **568**, 373–377 (2019)
78. Y. Hu et al., High-efficiency and broadband on-chip electro-optic frequency comb generators. Nat. Photonics **16**, 679–685 (2022)
79. K.-P. Ho, J.M. Kahn, Optical frequency comb generator using phase modulation in amplified circulating loop. IEEE Photonics Technol. Lett. **5**, 721–725 (1993)
80. Y. Sun et al., Applications of optical microcombs. Adv. Opt. Photonics **15**, 86 (2023)
81. M. Peccianti et al., Demonstration of a stable ultrafast laser based on a nonlinear microcavity. Nat. Commun. **3**, 765 (2012)
82. P. Haye, S.B. Papp, S.A. Diddams, Hybrid Electro-optically modulated microcombs. Phys. Rev. Lett. **109**, 263901 (2012)
83. A. Dutt et al., On-chip dual-comb source for spectroscopy. Sci. Adv. **4**, e1701858 (2018)
84. H. Guo et al., Universal dynamics and deterministic switching of dissipative Kerr solitons in optical microresonators. Nat. Phys. **13**, 94–102 (2017)
85. E. Obrzud, S. Lecomte, T. Herr, Temporal solitons in microresonators driven by optical pulses. Nat. Photonics **11**, 600–607 (2017)
86. B. Shen et al., Integrated turnkey soliton microcombs. Nature **582**, 365–369 (2020)
87. K. Jia et al., Automated turnkey microcomb for low-noise microwave synthesis. ArXiv arXiv **2211**, 10031 (2022)
88. M. Rowley et al., Self-emergence of robust solitons in a microcavity. Nature **608**, 303–309 (2022)
89. H. Bao et al., Laser cavity-soliton microcombs. Nat. Photonics **13**, 384–389 (2019)
90. M. Nie et al., Dissipative soliton generation and real-time dynamics in microresonator-filtered fiber lasers. Light Sci. Appl. **11**, 296 (2022)
91. B. Yao et al., Graphene-enhanced brillouin optomechanical microresonator for ultrasensitive gas detection. Nano Lett. **17**, 4996–5002 (2017)
92. K. Jia et al., Photonic flywheel in a monolithic fiber resonator. Phys. Rev. Lett. **125**, 143902 (2020)
93. Y. Bai et al., Brillouin-Kerr soliton frequency combs in an optical microresonator. Phys. Rev. Lett. **126**, 063901 (2021)
94. I.H. Do et al., Self-stabilized soliton generation in a microresonator through mode-pulled Brillouin lasing. Opt. Lett. **46**, 1772 (2021)
95. T. Tan et al., Multispecies and individual gas molecule detection using Stokes solitons in a graphene over-modal microresonator. Nat. Commun. **12**, 6716 (2021)
96. A.W. Bruch et al., Pockels soliton microcomb. Nat. Photonics **15**, 21–27 (2021)
97. X. Guo et al., Ultra-wideband integrated photonic devices on silicon platform: from visible to mid-IR. Nanophotonics **12**, 167–196 (2023)
98. V. Brasch et al., Photonic chip-based optical frequency comb using soliton Cherenkov radiation. Science **351**, 357–360 (2016)
99. C. Wang et al., High energy and low noise soliton fiber laser comb based on nonlinear merging of Kelly sidebands. Opt. Express **30**, 23556 (2022)
100. S. Zhang, J.M. Silver, T. Bi, Spectral extension and synchronization of microcombs in a single microresonator. Nat. Commun. **11**, 6384 (2020)
101. P.C. Qureshi et al., Soliton linear-wave scattering in a Kerr microresonator. Commun. Phys. **5**, 123 (2022)

102. H. Weng et al., Directly accessing octave-spanning dissipative Kerr soliton frequency combs in an AlN microresonator. Photonics Res. **9**, 1351 (2021)
103. Z. Xiao et al., Near-zero-dispersion soliton and broadband modulational instability Kerr microcombs in anomalous dispersion. Light Sci. Appl. **12**, 33 (2023)
104. G. Moille et al., Ultra-broadband Kerr microcomb through soliton spectral translation. Nat. Commun. **12**, 7275 (2021)
105. Q.-F. Yang, X. Yi, K.Y. Yang, K. Vahala, Stokes solitons in optical microcavities. Nat. Phys. **13**, 53–57 (2017)
106. X. Liu et al., Integrated high- Q Crystalline AlN microresonators for broadband kerr and raman frequency combs. ACS Photonics **5**, 1943–1950 (2018)
107. D. Xia et al., Engineered raman lasing in photonic integrated chalcogenide microresonators. Laser Photon. Rev. **16**, 2100443 (2022)
108. X. Jiang et al., Chaos-assisted broadband momentum transformation in optical microresonators. Science. **358**, 344–347 (2017)
109. X. Xue, P. Wang, Y. Xuan, M. Qi, A.M. Weiner, Microresonator Kerr frequency combs with high conversion efficiency. Laser Photon. Rev. **11**, 1600276 (2017)
110. X. Xue, X. Zheng, B. Zhou, Super-efficient temporal solitons in mutually coupled optical cavities. Nat. Photonics **13**, 616–622 (2019)
111. D.C. Cole, E.S. Lamb, Soliton crystals in Kerr resonators. Nat. Photonics **11**, 671–676 (2017)
112. Ó.B. Helgason et al., Surpassing the nonlinear conversion efficiency of soliton microcombs. Nat. Photonics **17**, 992–999 (2023)
113. M.H. Anderson et al., Photonic chip-based resonant supercontinuum via pulse-driven Kerr microresonator solitons. Optica **8**, 771 (2021)
114. Ó.B. Helgason et al., Dissipative solitons in photonic molecules. Nat. Photonics **15**, 305–310 (2021)
115. N. Englebert, C. Mas Arabí, P. Parra-Rivas, S.-P. Gorza, F. Leo, Temporal solitons in a coherently driven active resonator. Nat. Photonics **15**, 536–541 (2021)
116. Tan, T. *et al.* Gain-assisted microcomb dual-soliton manipulation. in *Conference on Lasers and Electro-Optics* STu1D5 (Optica Publishing Group, 2021). https://doi.org/10.1364/CLEO_SI.2021.STu1D.5.
117. M. Xu, M. He, Y. Zhu, S. Yu, X. Cai, Flat optical frequency comb generator based on integrated lithium niobate modulators. J. Light. Technol. **40**, 339–345 (2022)
118. C. Wang et al., Monolithic lithium niobate photonic circuits for Kerr frequency comb generation and modulation. Nat. Commun. **10**, 978 (2019)
119. Y. Wang et al., Noise canceled graphene-microcavity fiber laser sensor for ultrasensitive gas detection. Photonics Res. **11**, A1 (2023)
120. N. An et al., Brillouin lasers in a graphene microresonator for multispecies and individual gas molecule detection. APL Photonics **8**, 100801 (2023)
121. G. Lihachev et al., Low-noise frequency-agile photonic integrated lasers for coherent ranging. Nat. Commun. **13**, 3522 (2022)
122. C. Qin et al., Co-generation of orthogonal soliton pair in a monolithic fiber resonator with mechanical tunability. Laser Photon. Rev. **17**, 2200662 (2023)
123. Z. Lu et al., Synthesized soliton crystals. Nat. Commun. **12**, 3179 (2021)
124. T.E. Drake, J.R. Stone, T.C. Briles, S.B. Papp, Thermal decoherence and laser cooling of Kerr microresonator solitons. Nat. Photonics **14**, 480–485 (2020)
125. S. Zhu et al., Controllable Kerr and Raman-Kerr frequency combs in functionalized microsphere resonators. Nanophotonics **8**, 2321–2329 (2019)
126. K. Sengupta, T. Nagatsuma, D.M. Mittleman, Terahertz integrated electronic and hybrid electronic–photonic systems. Nat. Electron. **1**, 622–635 (2018)
127. A. Maestrini et al., A frequency-multiplied source with more than 1 mW of power across the 840–900-GHz Band. IEEE Trans. Microw. Theory Tech. **58**, 1925–1932 (2010)
128. K.A. McIntosh et al., Terahertz photomixing with diode lasers in low-temperature-grown GaAs. Appl. Phys. Lett. **67**, 3844–3846 (1995)
129. B.S. Williams, Terahertz quantum-cascade lasers. Nat. Photonics **1**, 517–525 (2007)
130. P. Chevalier et al., Widely tunable compact terahertz gas lasers. Science **366**, 856–860 (2019)
131. Y.Y. Choporova et al., High-power Bessel beams with orbital angular momentum in the terahertz range. Phys. Rev. A **96**, 023846 (2017)
132. O. Momeni, E. Afshari, High power Terahertz and millimeter-wave oscillator design: a systematic approach. IEEE J. Solid-State Circuits **46**, 583–597 (2011)
133. G.J. Schneider, J.A. Murakowski, C.A. Schuetz, S. Shi, D.W. Prather, Radiofrequency signal-generation system with over seven octaves of continuous tuning. Nat. Photonics **7**, 118–122 (2013)
134. T. Tetsumoto et al., Optically referenced 300 GHz millimetre-wave oscillator. Nat. Photonics **15**, 516–522 (2021)
135. B. Wang et al., Towards high-power, high-coherence, integrated photonic mmWave platform with microcavity solitons. Light Sci. Appl. **10**, 4 (2021)
136. W. Shao et al., Terabit FSO communication based on a soliton microcomb. Photonics Res. **10**, 2802 (2022)
137. G.K.M. Hasanuzzaman, S. Iezekiel, A. Kanno, W-band optoelectronic oscillator. IEEE Photonics Technol. Lett. **32**, 771–774 (2020)
138. J. Li, X. Yi, H. Lee, S.A. Diddams, K.J. Vahala, Electro-optical frequency division and stable microwave synthesis. Science **345**, 309–313 (2014)
139. W. Liang et al., High spectral purity Kerr frequency comb radio frequency photonic oscillator. Nat. Commun. **6**, 7957 (2015)
140. T.M. Fortier et al., Generation of ultrastable microwaves via optical frequency division. Nat. Photonics **5**, 425–429 (2011)
141. X. Xie et al., Photonic microwave signals with zeptosecond-level absolute timing noise. Nat. Photonics **11**, 44–47 (2017)
142. S. Gundavarapu et al., Sub-hertz fundamental linewidth photonic integrated Brillouin laser. Nat. Photonics **13**, 60–67 (2019)
143. W. Jin et al., Hertz-linewidth semiconductor lasers using CMOS-ready ultra-high-Q microresonators. Nat. Photonics **15**, 346–353 (2021)
144. G. Moille et al., Kerr-induced synchronization of a cavity soliton to an optical reference. Nature **624**, 267–274 (2023)
145. W. Wang et al., Coherent terahertz radiation with 2.8-octave tunability through chip-scale photomixed microresonator optical parametric oscillation. Nat. Commun. **13**, 5123 (2022)
146. J. Guo et al., Chip-based laser with 1-hertz integrated linewidth. Sci. Adv. **8**, eaab9006 (2022)
147. M.A. Tran et al., Extending the spectrum of fully integrated photonics to submicrometre wavelengths. Nature **610**, 54–60 (2022)
148. L.-S. Ma et al., Optical frequency synthesis and comparison with uncertainty at the 10–19 Level. Science. **303**, 1843–1845 (2004)
149. P. Del'Haye et al., Phase-coherent microwave-to-optical link with a self-referenced microcomb. Nat. Photonics. **10**, 516–520 (2016)
150. M. Chauvet et al., High efficiency frequency doubling in fully diced LiNbO 3 ridge waveguides on silicon. J. Opt. **18**, 085503 (2016)
151. S.-W. Huang et al., A broadband chip-scale optical frequency synthesizer at 2.7 × 10–16 relative uncertainty. Sci. Adv. **2**, 1501489 (2016)
152. M. Xin et al., Optical frequency synthesizer with an integrated erbium tunable laser. Light Sci. Appl. **8**, 122 (2019)
153. N. Singh et al., Silicon photonics optical frequency synthesizer. Laser Photon. Rev. **14**, 1900449 (2020)
154. I. Kudelin et al., Photonic chip-based low-noise microwave oscillator. Nature **627**, 534–539 (2024)
155. S. Sun et al., Integrated optical frequency division for microwave and mmWave generation. Nature **627**, 540–545 (2024)
156. Y. Zhao et al., All-optical frequency division on-chip using a single laser. Nature **627**, 546–552 (2024)
157. G. Rademacher et al., Peta-bit-per-second optical communications system using a standard cladding diameter 15-mode fiber. Nat. Commun. **12**, 4238 (2021)
158. H. Kaushal, G. Kaddoum, Optical communication in space: challenges and mitigation techniques. IEEE Commun. Surv. Tutorials **19**, 57–96 (2017)
159. S. Okamoto et al., A study on the effect of ultra-wide band WDM on optical transmission systems. J. Light. Technol. **38**, 1061–1070 (2020)
160. I. Roudas et al., Optimal polarization demultiplexing for coherent optical communications systems. J. Light. Technol. **28**, 1121–1134 (2010)
161. J. Wang et al., Terabit free-space data transmission employing orbital angular momentum multiplexing. Nat. Photonics **6**, 488–496 (2012)
162. Z. Wang et al., Room-temperature InP distributed feedback laser array directly grown on silicon. Nat. Photonics **9**, 837–842 (2015)

163. Kabir, W. Orthogonal Frequency Division Multiplexing (OFDM). *2008 China-Japan Joint Microwave Conference* 178–184 (IEEE, 2008). https://doi.org/10.1109/CJMW.2008.4772401.
164. M.A. Soto et al., Optical sinc-shaped Nyquist pulses of exceptional quality. Nat. Commun. **4**, 2898 (2013)
165. Puttnam, B. J. *et al*. 215 Pb/s transmission using a 22 core homogeneous single-mode multi-core fiber and wideband optical comb. European Conference on Optical Communication (ECOC) 1–3 (IEEE, 2015). https://doi.org/10.1109/ECOC.2015.7341685.
166. R. Zhuang et al., Electro-Optic Frequency Combs: Theory, Characteristics, and Applications. Laser Photon. Rev. **17**, 2200353 (2023)
167. P. Marin-Palomo et al., Microresonator-based solitons for massively parallel coherent optical communications. Nature **546**, 274–279 (2017)
168. Y. Geng et al., Coherent optical communications using coherence-cloned Kerr soliton microcombs. Nat. Commun. **13**, 1070 (2022)
169. K.Y. Yang et al., Multi-dimensional data transmission using inverse-designed silicon photonics and microcombs. Nat. Commun. **13**, 7862 (2022)
170. A.A. Jørgensen et al., Petabit-per-second data transmission using a chip-scale microcomb ring resonator source. Nat. Photonics **16**, 798–802 (2022)
171. A. Fülöp et al., High-order coherent communications using mode-locked dark-pulse Kerr combs from microresonators. Nat. Commun. **9**, 1598 (2018)
172. L. Lundberg et al., Phase-coherent lightwave communications with frequency combs. Nat. Commun. **11**, 201 (2020)
173. Y. Geng et al., Terabit optical OFDM superchannel transmission via coherent carriers of a hybrid chip-scale soliton frequency comb. Opt. Lett. **43**, 2406 (2018)
174. B. Corcoran et al., Ultra-dense optical data transmission over standard fibre with a single chip source. Nat. Commun. **11**, 2568 (2020)
175. A.S. Raja et al., Ultrafast optical circuit switching for data centers using integrated soliton microcombs. Nat. Commun. **12**, 5867 (2021)
176. M. Corato-Zanarella et al., Widely tunable and narrow-linewidth chip-scale lasers from near-ultraviolet to near-infrared wavelengths. Nat. Photonics **17**, 157–164 (2023)
177. J. Liu et al., Ultralow-power chip-based soliton microcombs for photonic integration. Optica **5**, 1347 (2018)
178. A. Rizzo et al., Massively scalable Kerr comb-driven silicon photonic link. Nat. Photonics **17**, 781–790 (2023)
179. T. Ishibashi, H. Ito, Uni-traveling carrier photodiodes: development and prospects. IEEE J. Sel. Top. Quantum Electron. **28**, 1–6 (2022)
180. Y. Lin et al., Monolithically integrated, broadband, high-efficiency silicon nitride-on-silicon waveguide photodetectors in a visible-light integrated photonics platform. Nat. Commun. **13**, 6362 (2022)
181. B.M. Heffernan et al., 60 Gbps real-time wireless communications at 300 GHz carrier using a Kerr microcomb-based source. APL Photonics **8**, 066106 (2023)
182. G. Kurizki et al., Quantum technologies with hybrid systems. Proc. Natl. Acad. Sci. **112**, 3866–3873 (2015)
183. Z. Xie et al., Harnessing high-dimensional hyperentanglement through a biphoton frequency comb. Nat. Photonics **9**, 536–542 (2015)
184. M. Kues et al., Quantum optical microcombs. Nat. Photonics **13**, 170–179 (2019)
185. L. Caspani et al., Integrated sources of photon quantum states based on nonlinear optics. Light Sci. Appl. **6**, e17100–e17100 (2017)
186. T.J. Steiner, M. Shen, J.E. Castro, J.E. Bowers, G. Moody, Continuous entanglement distribution from an AlGaAs-on-insulator microcomb for quantum communications. Opt. Quantum **1**, 55 (2023)
187. F. Mazeas et al., High-quality photonic entanglement for wavelength-multiplexed quantum communication based on a silicon chip. Opt. Express **24**, 28731 (2016)
188. B.-H. Wu, R.N. Alexander, S. Liu, Z. Zhang, Quantum computing with multidimensional continuous-variable cluster states in a scalable photonic platform. Phys. Rev. Res. **2**, 023138 (2020)
189. Y.K. Chembo, Quantum dynamics of Kerr optical frequency combs below and above threshold: spontaneous four-wave mixing, entanglement, and squeezed states of light. Phys. Rev. A **93**, 033820 (2016)
190. C. Reimer et al., Integrated frequency comb source of heralded single photons. Opt. Express **22**, 6535 (2014)
191. C. Reimer et al., Generation of multiphoton entangled quantum states by means of integrated frequency combs. Science **351**, 1176–1180 (2016)
192. M. Kues et al., On-chip generation of high-dimensional entangled quantum states and their coherent control. Nature **546**, 622–626 (2017)
193. H.-H. Lu et al., Bayesian tomography of high-dimensional on-chip biphoton frequency combs with randomized measurements. Nat. Commun. **13**, 4338 (2022)
194. Y. Fan et al., Multi-wavelength quantum light sources on silicon nitride micro-ring chip. Laser Photon. Rev. **17**, 2300172 (2023)
195. C. Wang et al., Integrated high quality factor lithium niobate microdisk resonators. Opt. Express **22**, 30924 (2014)
196. K.-H. Luo et al., Nonlinear integrated quantum electro-optic circuits. Sci. Adv. **5**, eaat1451 (2019)
197. F. Lenzini et al., Integrated photonic platform for quantum information with continuous variables. Sci. Adv. **4**, eaat9331 (2018)
198. Z. Ma et al., Ultrabright quantum photon sources on chip. Phys. Rev. Lett. **125**, 263602 (2020)
199. G.-T. Xue et al., Ultrabright multiplexed energy-time-entangled photon generation from lithium niobate on insulator chip. Phys. Rev. Appl. **15**, 064059 (2021)
200. M.A. Guidry, D.M. Lukin, K.Y. Yang, R. Trivedi, J. Vučković, Quantum optics of soliton microcombs. Nat. Photonics **16**, 52–58 (2022)
201. J. Suo, W. Zhang, S. Dong, Y. Huang, J. Peng, Discrete frequency entangled photon pair generation based on silicon micro-ring cavities. J. Phys. Soc. Japan **85**, 104401 (2016)
202. Z. Yang et al., A squeezed quantum microcomb on a chip. Nat. Commun. **12**, 4781 (2021)
203. M. Jahanbozorgi et al., Generation of squeezed quantum microcombs with silicon nitride integrated photonic circuits. Optica **10**, 1100 (2023)
204. B. Stern, X. Ji, Y. Okawachi, A.L. Gaeta, M. Lipson, Battery-operated integrated frequency comb generator. Nature **562**, 401–405 (2018)
205. A.S. Raja et al., Electrically pumped photonic integrated soliton microcomb. Nat. Commun. **10**, 680 (2019)
206. F. Samara et al., Entanglement swapping between independent and asynchronous integrated photon-pair sources. Quantum Sci. Technol. **6**, 045024 (2021)
207. W. Wen et al., Realizing an entanglement-based multiuser quantum network with integrated photonics. Phys. Rev. Appl. **18**, 024059 (2022)
208. S.A. Diddams, L. Hollberg, V. Mbele, Molecular fingerprinting with the resolved modes of a femtosecond laser frequency comb. Nature **445**, 627–630 (2007)
209. B. Lomsadze, S.T. Cundiff, Frequency combs enable rapid and high-resolution multidimensional coherent spectroscopy. Science **357**, 1389–1391 (2017)
210. T. Ideguchi, A. Poisson, G. Guelachvili, N. Picqué, T.W. Hänsch, Adaptive real-time dual-comb spectroscopy. Nat. Commun. **5**, 3375 (2014)
211. G. Millot et al., Frequency-agile dual-comb spectroscopy. Nat. Photonics **10**, 27–30 (2016)
212. M.-G. Suh, Q.-F. Yang, K.Y. Yang, X. Yi, K.J. Vahala, Microresonator soliton dual-comb spectroscopy. Science **354**, 600–603 (2016)
213. M. Yu et al., Silicon-chip-based mid-infrared dual-comb spectroscopy. Nat. Commun. **9**, 1869 (2018)
214. L. Stern et al., Direct Kerr frequency comb atomic spectroscopy and stabilization. Sci. Adv. **6**, 6230 (2020)
215. C. Bao et al., Architecture for microcomb-based GHz-mid-infrared dual-comb spectroscopy. Nat. Commun. **12**, 6573 (2021)
216. A. Shams-Ansari et al., Thin-film lithium-niobate electro-optic platform for spectrally tailored dual-comb spectroscopy. Commun. Phys. **5**, 88 (2022)
217. P. Trocha et al., Ultrafast optical ranging using microresonator soliton frequency combs. Science **359**, 887–891 (2018)
218. M.G. Suh, K.J. Vahala, Soliton microcomb range measurement. Science **359**, 884–887 (2018)
219. Y.S. Jang et al., Nanometric precision distance metrology via hybrid spectrally resolved and homodyne interferometry in a single soliton frequency microcomb. Phys. Rev. Lett. **126**, 23903 (2021)
220. J. Riemensberger et al., Massively parallel coherent laser ranging using a soliton microcomb. Nature **581**, 164–170 (2020)

221. A. Lukashchuk, J. Riemensberger, M. Karpov, J. Liu, T.J. Kippenberg, Dual chirped microcomb based parallel ranging at megapixel-line rates. Nat. Commun. **13**, 3280 (2022)
222. J. Wang et al., Long-distance ranging with high precision using a soliton microcomb. Photonics Res. **8**, 1964 (2020)
223. J. Zheng et al., Optical ranging system based on multiple pulse train interference using soliton microcomb. Appl. Phys. Lett. **118**, 261106 (2021)
224. R. Chen et al., Breaking the temporal and frequency congestion of LiDAR by parallel chaos. Nat. Photonics **17**, 306–314 (2023)
225. A. Lukashchuk, J. Riemensberger, A. Tusnin, J. Liu, T.J. Kippenberg, Chaotic microcomb-based parallel ranging. Nat. Photonics **17**, 814–821 (2023)
226. M. Karpov, M.H.P. Pfeiffer, J. Liu, A. Lukashchuk, T.J. Kippenberg, Photonic chip-based soliton frequency combs covering the biological imaging window. Nat. Commun. **9**, 1146 (2018)
227. X. Ji et al., Chip-based frequency comb sources for optical coherence tomography. Opt. Express **27**, 19896 (2019)
228. P.J. Marchand et al., Soliton microcomb based spectral domain optical coherence tomography. Nat. Commun. **12**, 427 (2021)
229. C. Bao, M.-G. Suh, K. Vahala, Microresonator soliton dual-comb imaging. Optica **6**, 1110 (2019)
230. E. Vicentini, Z. Wang, K. Van Gasse, T.W. Hänsch, N. Picqué, Dual-comb hyperspectral digital holography. Nat. Photonics **15**, 890–894 (2021)
231. N. An et al., Graphene-fiber biochemical sensors: principles, implementations, and advances. Photonic Sensors **11**, 123–139 (2021)
232. Y. Guo et al., Optical microcavities empowered biochemical sensing: status and prospects. Adv. Devices Instrum. **5**, 0441 (2024)
233. M. Knoerzer et al., Optical frequency comb based system for photonic refractive index sensor interrogation. Opt. Express **27**, 21532 (2019)
234. Z. Cao et al., Biochemical sensing in graphene-enhanced microfiber resonators with individual molecule sensitivity and selectivity. Light Sci. Appl. **8**, 107 (2019)
235. Y. Liang et al., Harnessing sub-comb dynamics in a graphene-sensitized microresonator for gas detection. Front. Optoelectron. **17**, 12 (2024)
236. N. An et al., Electrically tunable four-wave-mixing in graphene heterogeneous fiber for individual gas molecule detection. Nano Lett. **20**, 6473–6480 (2020)
237. J. Zhang et al., Optomechanical dissipative solitons. Nature **600**, 75–80 (2021)
238. M. Soriano-Amat et al., Time-expanded phase-sensitive optical time-domain reflectometry. Light Sci. Appl. **10**, 51 (2021)
239. X.-H. Jia, H.-Q. Chang, K. Lin, C. Xu, J.-G. Wu, Frequency-comb-based BOTDA sensors for high-spatial-resolution/long-distance sensing. Opt. Express **25**, 6997 (2017)
240. J.-T. Li et al., Coherently parallel fiber-optic distributed acoustic sensing using dual Kerr soliton microcombs. Sci. Adv. **10**, 8666 (2024)
241. R. Nagarajan et al., Large-scale photonic integrated circuits. IEEE J. Sel. Top. Quantum Electron. **11**, 50–65 (2005)
242. D. Marpaung, J. Yao, J. Capmany, Integrated microwave photonics. Nat. Photonics **13**, 80–90 (2019)
243. C. Haffner et al., All-plasmonic Mach-Zehnder modulator enabling optical high-speed communication at the microscale. Nat. Photonics **9**, 525–528 (2015)
244. W. Heni et al., Silicon-organic and plasmonic-organic hybrid photonics. ACS Photonics **4**, 1576–1590 (2017)
245. J. Riemensberger et al., A photonic integrated continuous-travelling-wave parametric amplifier. Nature **612**, 56–61 (2022)
246. C. Liu et al., Silicon/2D-material photodetectors: from near-infrared to mid-infrared. Light Sci. Appl. **10**, 123 (2021)
247. R. Pant et al., On-chip stimulated brillouin scattering for microwave signal processing and generation. Laser Photon. Rev. **8**, 653–666 (2014)
248. J.-H. Kim, S. Aghaeimeibodi, J. Carolan, D. Englund, E. Waks, Hybrid integration methods for on-chip quantum photonics. Optica **7**, 291 (2020)
249. J.-H. Kang et al., Monolithic 3D integration of 2D materials-based electronics towards ultimate edge computing solutions. Nat. Mater. **22**, 1470–1477 (2023)
250. L. Zhuang, C.G.H. Roeloffzen, M. Hoekman, K.-J. Boller, A.J. Lowery, Programmable photonic signal processor chip for radiofrequency applications. Optica **2**, 854 (2015)
251. D. Pérez et al., Multipurpose silicon photonics signal processor core. Nat. Commun. **8**, 636 (2017)
252. J. Capmany, I. Gasulla, D. Pérez, The programmable processor. Nat. Photonics **10**, 6–8 (2016)
253. W. Liu et al., A fully reconfigurable photonic integrated signal processor. Nat. Photonics **10**, 190–195 (2016)
254. J. Liu et al., Photonic microwave generation in the X- and K-band using integrated soliton microcombs. Nat. Photonics **14**, 486–491 (2020)
255. J. Hu et al., Reconfigurable radiofrequency filters based on versatile soliton microcombs. Nat. Commun. **11**, 4377 (2020)
256. X. Xue et al., Microcomb-based true-time-delay network for microwave beamforming with arbitrary beam pattern control. J. Light. Technol. **36**, 2312–2321 (2018)
257. F. Ferdous et al., Spectral line-by-line pulse shaping of on-chip microresonator frequency combs. Nat. Photonics **5**, 770–776 (2011)
258. X. Xu et al., Broadband RF channelizer based on an integrated optical frequency kerr comb source. J. Light. Technol. **36**, 4519–4526 (2018)
259. M. Tan et al., Photonic signal processor based on a Kerr microcomb for real-time video image processing. Commun. Eng. **2**, 94 (2023)
260. X. Xue et al., Programmable single-bandpass photonic rf filter based on Kerr Comb from a Microring. J. Light. Technol. **32**, 3557–3565 (2014)
261. J. Wu et al., RF photonics: an optical microcombs' perspective. IEEE J. Sel. Top. Quantum Electron. **24**, 1–20 (2018)
262. X. Xu et al., Reconfigurable broadband microwave photonic intensity differentiator based on an integrated optical frequency comb source. APL Photonics **2**, 096104 (2017)
263. M. Tan et al., Highly versatile broadband RF photonic fractional Hilbert transformer based on a kerr soliton crystal microcomb. J. Light. Technol. **39**, 7581–7587 (2021)
264. X. Xu et al., High performance RF filters via bandwidth scaling with Kerr micro-combs. APL Photonics **4**, 026102 (2019)
265. Q.-F. Yang et al., Dispersive-wave induced noise limits in miniature soliton microwave sources. Nat. Commun. **12**, 1442 (2021)
266. Tan, M. *et al.* Photonic microwave and RF channelizers based on Kerr micro-combs. in Terahertz, RF, Millimeter, and submillimeter-wave technology and applications XIV (eds. Sadwick, L. P. & Yang, T.) 22 (SPIE, 2021). (2021). https://doi.org/10.1117/12.2584015.
267. B. Yao et al., Broadband gate-tunable terahertz plasmons in graphene heterostructures. Nat. Photonics **12**, 22–28 (2018)
268. O. Dogadov, C. Trovatello, B. Yao, G. Soavi, G. Cerullo, Parametric nonlinear optics with layered materials and related heterostructures. Laser Photon. Rev. **16**, 2100726 (2022)
269. J. Kono, Coherent terahertz control. Nat. Photonics **5**, 5–6 (2011)
270. L. Wang et al., Ultrafast terahertz transparency boosting in graphene meta-cavities. Nanophotonics **11**, 4899–4907 (2022)
271. X. Guo et al., Efficient generation of a near-visible frequency comb via cherenkov-like radiation from a kerr microcomb. Phys. Rev. Appl. **10**, 014012 (2018)
272. H. Zhang et al., Soliton microcombs multiplexing using intracavity-stimulated brillouin lasers. Phys. Rev. Lett. **130**, 153802 (2023)
273. C. Bao et al., Interleaved difference-frequency generation for microcomb spectral densification in the mid-infrared. Optica **7**, 309 (2020)
274. Y. Li et al., Nonlinear co-generation of graphene plasmons for optoelectronic logic operations. Nat. Commun. **13**, 3138 (2022)
275. P.L. McMahon, The physics of optical computing. Nat. Rev. Phys. **5**, 717–734 (2023)
276. Y. Okawachi, B.Y. Kim, M. Lipson, A.L. Gaeta, Chip-scale frequency combs for data communications in computing systems. Optica **10**, 977 (2023)
277. J. Feldmann et al., Parallel convolutional processing using an integrated photonic tensor core. Nature **589**, 52–58 (2021)
278. X. Xu et al., 11 TOPS photonic convolutional accelerator for optical neural networks. Nature **589**, 44–51 (2021)
279. B. Bai et al., Microcomb-based integrated photonic processing unit. Nat. Commun. **14**, 66 (2023)
280. J. Cheng et al., Human emotion recognition with a microcomb-enabled integrated optical neural network. Nanophotonics **12**, 3883–3894 (2023)
281. K. Takahashi, H. Matsui, T. Nagashima, T. Konishi, Resolution upgrade toward 6-bit optical quantization using power-to-wavelength conversion for photonic analog-to-digital conversion. Opt. Lett. **38**, 4864 (2013)

282. A.E. Willner, A. Fallahpour, K. Zou, F. Alishahi, H. Zhou, Optical signal processing aided by optical frequency combs. IEEE J. Sel. Top. Quantum Electron. **27**, 1–16 (2021)
283. Y. Liu et al., A photonic integrated circuit–based erbium-doped amplifier. Science **376**, 1309–1313 (2022)
284. F.C. Cruz, M.C. Stowe, J. Ye, Tapered semiconductor amplifiers for optical frequency combs in the near infrared. Opt. Lett. **31**, 1337 (2006)
285. K. Wu et al., Vernier microcombs for high-frequency carrier envelope offset and repetition rate detection. Optica **10**, 626 (2023)
286. T. Wildi, A. Ulanov, N. Englebert, T. Voumard, T. Herr, Sideband injection locking in microresonator frequency combs. APL Photonics **8**, 120801 (2023)
287. J. Lu et al., Periodically poled thin-film lithium niobate microring resonators with a second-harmonic generation efficiency of 250,000%/W. Optica **6**, 1455 (2019)
288. T. Tan et al., Gain-assisted chiral soliton microcombs. Arxiv arXiv **2008**, 122150 (2008)
289. D. Luo et al., 130 W, 180 fs ultrafast Yb-doped fiber frequency comb based on chirped-pulse fiber amplification. Opt. Express **28**, 4817 (2020)
290. Q. Guo et al., Ultrafast mode-locked laser in nanophotonic lithium niobate. Science. **382**, 708–713 (2023)
291. A.E. Ulanov et al., Synthetic reflection self-injection-locked microcombs. Nat Photonics **18**, 294–299 (2024)
292. C. Xiang et al., Laser soliton microcombs heterogeneously integrated on silicon. Science. **373**, 99–103 (2021)
293. Q. Li et al., Stably accessing octave-spanning microresonator frequency combs in the soliton regime. Optica **4**, 193 (2017)
294. B. Meng et al., Mid-infrared frequency comb from a ring quantum cascade laser. Optica **7**, 162 (2020)
295. K. Zhang et al., A power-efficient integrated lithium niobate electro-optic comb generator. Commun. Phys. **6**, 17 (2023)
296. Ji, X. et al. 2023. A Photonic Integrated High-power Soliton Microcomb Generator in CLEO 2023 SW4L1. https://doi.org/10.1364/CLEO_SI.2023.SW4L.1.